https://doi.org/10.5194/bg-2020-11
Preprint. Discussion started: 3 February 2020

Biogeosciences Discussions
Open Access
EGU

Microbial communities associated with sediments and polymetallic nodules of the Peru Basin

Massimiliano Molari[1], Felix Janssen[1,2], Tobias Vonnahme[1,a], Frank Wenzhöfer[1,2] and Antje Boetius[1,2]

[1] Max Planck Institute for Marine Microbiology, Bremen, Germany
[2] HGF-MPG Joint Research Group on Deep Sea Ecology and Technology, Alfred Wegener Institute for Polar and Marine Research, Bremerhaven, Germany

[a] Present address: UiT the Arctic University of Tromsø, Tromsø, Norway

Correspondence to: Massimiliano Molari (mamolari@mpi-bremen.de)

https://doi.org/10.5194/bg-2020-11
Preprint. Discussion started: 3 February 2020

Biogeosciences Discussions
Open Access

Abstract. Industrial-scale mining of deep-sea polymetallic nodules will need to remove nodules in large areas of the seafloor. The regrowth of the nodules by metal precipitation is estimated to take millions of years. Thus for future mining impact studies, it is crucial to understand the role of nodules in shaping microbial diversity and function in deep-sea environments. Here we investigated microbial community composition based on 16S rRNA gene sequences retrieved from sediments and nodules of the Peru Basin (>4100 m water depth). The nodule field of the Peru Basin showed a typical deep-sea microbiome, with dominance of the classes Gammaproteobacteria, Alphaproteobacteria, Deltaproteobacteria, and Acidimicrobiia. Nodules and sediments host distinct bacterial and archaeal communities, with nodules showing lower diversity and a higher proportion of sequences related to potential metal-cycling bacteria (i.e. Magnetospiraceae, Hyphomicrobiaceae), bacterial and archaeal nitrifiers (i.e. *AqS1*, unclassified Nitrosomonadaceae, *Nitrosopumilus*, *Nitrospina*, *Nitrospira*), and bacterial sequences found in ocean crust, nodules, hydrothermal deposits and sessile fauna. Sediment and nodule communities overall shared a low proportion of Operational Taxonomic Units (OTU; 21 % for Bacteria and 19 % for Archaea). Our results show that nodules represent a specific ecological niche (i.e. hard substrate, high metal concentrations and sessile fauna), with a potentially relevant role in organic carbon degradation. Differences in nodule community composition (e.g. Mn-cycling bacteria, nitrifiers) between the Clarion-Clipperton Fracture Zone (CCZ) and the Peru Basin suggest that changes in environmental setting (i.e. sedimentation rates) play also a significant role in structuring the nodule microbiome.

https://doi.org/10.5194/bg-2020-11
Preprint. Discussion started: 3 February 2020

1 Introduction

Polymetallic nodules (or manganese nodules) occur in abyssal plains (4000–6000 m water depth) and consist primarily of manganese and iron, as well as many other metals and rare earth elements (Crerar and Barnes, 1974; Kuhn et al. 2017). Nodules are potato- or cauliflower-shaped structures with typical diameters of 4–20 cm and are typically found at the sediment surface or occasionally buried in the uppermost 10 cm sediment horizon. The mechanisms of nodule formation are not completely elucidated. The current understanding is that they are formed via mineral precipitations from bottom waters (*Hydrogenetic* growth) or pore waters (*Diagenetic* growth) involving both abiotic and microbiological processes (Crerar and Barnes, 1974; Riemann, 1983; Halbach et al., 1988; Wang et al., 2009). The formation of nodules is a slow process that is estimated to range between thousands and millions of years per millimetre growth (Kerr, 1984; Boltenkov, 2012).

Rising global demand for metals has renewed interests in commercial mining of deep-sea nodule deposits. Mining operations would remove nodules, disturb or erode the top decimeters of sediment, and create near bottom sediment plumes that will resettle and cover the seafloor (Miller et al., 2018). Although the first nodules have been discovered in the 1870's (Murray, 1891), only little is known about the biodiversity, biological processes and ecological functions of the nodules and their surrounding sediments as specific deep-see habitat. Major questions remain, for example as to spatial turnover on local and global scales, the role of the microbial community in and around nodules, the role of nodules as substrate for endemic species. Hence, there is the need to thoroughly characterize baseline conditions as a requirement for any mining operations as these will require assessments of impacts associated with mining.

Extensive and dense nodule fields are found in different areas of the Pacific and Indian deep seas. Nodule accumulations of economic interest have been found in four geographical locations: the Clarion-Clipperton Fracture Zone (CCZ) and the Penrhyn Basin in the central north and south Pacific Ocean, respectively; the Peru Basin in the south-east Pacific; and in the center of the north Indian Ocean (Miller et al., 2018). Previous work on the structure of microbial communities of nodule fields by 16S rRNA gene sequencing focused on the CCZ and the central South Pacific Ocean (Xu et al., 2007; Wu et al., 2013; Tully and Heidelberg, 2013; Blöthe et al., 2015; Shulse et al., 2016; Lindh et al., 2017). All studies showed that polymetallic nodules harbor microorganisms that are distinct from the surrounding sediments and overlying water. They indicate that nodule communities show a pronounced spatial variability, but these results are so far not conclusive. Similar microbial communities were observed in nodules collected at distances of 6000 km and 30 km (Wu et al., 2013; Shulse et al. 2016), while Tully and Heidelberg (2013) found that nodule communities varied among sampling sites (<50 km). Besides, potential Mn-oxidizers and -reducers such as *Alteromonas*, *Pseudoalteromonas*, *Shewanella* and *Colwellia* were proposed as a core of the nodule microbiome involved in the formation of nodules (Wu et al. 2013; Blöthe et al., 2015), but they were not found in all nodules sampled so far (Tully and Heidelberg, 2013; Shulse et al. 2016). The lack of knowledge on the diversity and composition of microbial assemblages of other nodule provinces makes it difficult to assess whether observed differences within the CCZ may reflect regional differences in environmental conditions (e.g.

https://doi.org/10.5194/bg-2020-11
Preprint. Discussion started: 3 February 2020

input of organic matter, bathymetry, topography, sediment type), or in abundance and morphology of nodules, or in the colonization of the nodules by epifauna and protozoans.

In this study we investigated the diversity and composition of bacterial and archaeal communities associated with manganese nodule fields of the Peru Basin. The Peru Basin is located about 3000 km off the coast of Peru and covers about half of the size of the CCZ, which is 5.000–9.000 km away. The present-day organic carbon flux in this area is approximately two times higher than in the CCZ, resulting in higher content of organic carbon in the surface sediments (>1% *vs* 02−06% in the CCZ), and a shallower oxic-suboxic front (10 cm *vs* tens of meters sediments depth in the CCZ; Müller et al., 1988; Heakel et al., 2001; Volz et al., 2018). As a consequence of differences in environmental conditions (e.g. organic carbon flux, carbonate compensation depth, sediment type, topography and near-bottom currents), the Peru basin and the CCZ host manganese nodules with different geological features (Kuhn et al. 2017). This includes: i) nodules from the Peru Basin are often larger, with a typical cauliflower shape, compared to those in CCZ that have a discoidal shape and a size of 2-8 cm (Kuhn et al. 2017); ii) average nodule abundance in the Peru Basin is lower (10 kg m^{-2}) than in CCZ (15 kg m^{-2}; Kuhn et al. 2017); iii) Mn nodules from the Peru Basin are thought to be mainly formed by suboxic diagenesis, whereas CCZ nodules apparently exhibit a mixture of diagenetic and hydrogenetic origin (von Stackelberg 1997; Chester and Jickells 2012); iv) while Peru Basin and CCZ nodules consist of the same type of mineral (disordered phyllomanganates), they have a different metal content (Wegorzewski and Kuhn 2014; Wegorzewski et al. 2015).

An increasing number of studies and policy discussions address the scientific basis of ecological monitoring in deep-sea mining, highlighting the need to identify appropriate indicators and standards for environmental impact assessments and ecological management. A key aspect is avoiding harmful effects to the marine environment, which will have to include loss of species and ecosystem functions. The aims of this study was to assess the structure and similarity of benthic microbial communities of nodules and sediments of the Peru Basin nodule province, and to compare them with those of other global deep-sea sediments and nodules in the CCZ. The focus was on similarity comparisons in order to investigate endemism and potential functional taxa that could be lost due to the removal of manganese nodules by mining activities. To achieve this, the hypervariable 16S rRNA regions V3-V4 for Bacteria and, V3-V5 for Archaea were amplified from DNA extracted from nodules and surrounding sediments and sequenced using the Illumina paired-end MiSeq platform. The hypotheses tested were i) nodules shape deep-sea microbial diversity and functions, ii) nodules host specific microbial community compared to the surrounding sediments, and iii) environmental setting and nodule features impact microbial community composition.

https://doi.org/10.5194/bg-2020-11
Preprint. Discussion started: 3 February 2020

2 Methods

2.1 Sample collection

Sediment samples and polymetallic nodules were collected as a part of the MiningImpact project of the Joint Programming Initiative JPI Healthy and Productive Seas and Oceans (JPIOcean) on board of R/V Sonne (expedition SO242/2; 28th of August - 1st of October 2015) in the Peru Basin around 7° S and 88.5° W. Samples were collected at three sites outside the seafloor area selected in 1989 for a long-term disturbance and recolonization experiment (DISCOL; Thiel et al., 2001), for this reason they were called "References Sites". Sediment samples were collected using TV-guided MUltiple Corer (TV-MUC) at three stations per site (Table 1). The cores were sliced on board in a temperature-controlled room (set at *in situ* temperature), and aliquots of sediment were stored at −20 °C for DNA extraction and prepared for cell counts (see sections below). Manganese nodules where sampled, using a TV-MUC, or a Remotely Operated Vehicle (ROV Kiel6000). The nodules where partly located at the surface or buried down to 3 cm below the seafloor (bsf) with diameters of a few cm. Nodules were gently rinsed with 0.22-µm filtered cold bottom seawater to remove adhering sediment, stored in sterile plastic bags at −20 °C and crushed before DNA extraction in the home lab.

2.2 DNA extraction and sequencing

The nodules collected with the MUC where crushed and stored at −20 °C. From the nodules collected with the ROV, only the surface layer was scraped off using a sterile spoon, and subsequently crushed and frozen (−20 °C). The DNA was extracted from 1 g of wet sediment (0-1 cm layer) and from 1 g of wet nodule's fragments using the FastDNA™ SPIN Kit for Soil (Q-BIOgene, Heidelberg, Germany) following the manual protocol. An isopropanol precipitation was performed on the extracted DNA, and DNA samples were stored at −20 °C. As control for DNA contamination (negative control), DNA extraction was carried out on purified water after being in contact with sterile scalpel and plastic bag.

Amplicon sequencing was done at the CeBiTec laboratory (Centrum für Biotechnologie, Universität Bielefeld) on an Illumina MiSeq machine. For the 16S amplicon library preparation we used the bacterial primers 341F (5´-CCTACGGGNGGCWGCAG-3´) and 785R (5´-GACTACHVGGGTATC TAATCC-3´), and the archaeal primers Arch349F (5´-GYGCASCAGKCGMGAAW-3´) and Arch915R (5´-GTGCTCCCCCGCCAATTCCT-3´) (Wang and Qian, 2009; Klindworth et al., 2013), which amplify the 16S rDNA hypervariable region V3-V4 in Bacteria (400−425 bp fragment length) and the V3-V5 region in Archaea (510 bp fragment length). The amplicon library was sequenced with the MiSeq v3 chemistry, in a 2x300 bp paired run with >50,000 reads per sample, following the standard instructions of the 16S Metagenomic Sequencing Library Preparation protocol (Illumina, Inc., San Diego, CA, USA).

The quality cleaning of the sequences was performed with several software tools. CUTADAPT (Martin, 2011) was used for primer clipping. Subsequently the TRIMMOMATIC software (Bolger et al., 2014) was used to remove low-quality sequences (for Bacteria SLIDINGWINDOW:4:10 MINLEN:300; for Archaea SLIDINGWINDOW:6:13 MINLEN:450): In case of bacteria data this step was performed before the merging of reverse and forward reads with PEAR (Zhang et al., 2014) while merging of the archaeal data set was done after removing low-quality sequences in order to enhance the

https://doi.org/10.5194/bg-2020-11
Preprint. Discussion started: 3 February 2020

number of retained reads for long archaeal 16S fragments. Clustering of sequences into OTUs (operational taxonomic units) was done using the SWARM algorithm (Mahé et al., 2014). The taxonomic classification was based on the SILVA rRNA reference database (release 132), at a minimum alignment similarity of 0.9, and a last common ancestor consensus of 0.7 (Pruesse et al., 2012). Raw sequences with removed primer sequences were deposited at the European Nucleotide Archive (ENA) under accession number PRJEB30517 and PRJEB32680; the sequences were archived using the service of the German Federation for Biological Data (GFBio; Diepenbroek et al., 2014).

The total number of sequences obtained in this study is reported in table 2. Absolute singletons (SSOabs), i.e. OTUs consisting of sequences occurring only once in the full dataset (Gobet et al., 2013) were removed (Table 2). Similarly, contaminant sequences (as observed in the negative control) and unspecific sequences (i.e., bacterial sequences in the archaeal amplicon dataset, and archaeal, chloroplast, and mitochondrial sequences in the bacterial dataset) were removed from amplicon data sets before the analysis (Table 2). The dominant OTU sequences and OTU sequences highly abundant in the nodules were subjected to BLAST search (BLASTn; Gene Bank nucleotide database 12/06/2019) in order to identify in which others habitats the closest related (i.e. >99 %) sequences have been previously reported.

2.3 Data analysis

The first three Hill Numbers, or the effective number of species, were used to describe alpha-diversity: species richness (H_0), the exponential of Shannon entropy (H_1), and the inverse Simpson index (H_2; Chao et al., 2014). Coverage-based and sample-size-based rarefaction (based on actual number of sequences) and extrapolation (based on double number of sequences) curves were calculated for the Hill's numbers using the R package iNEXT (Hsieh et al., 2018). Calculation of the estimated richness (Chao1) and the identification of unique OTUs (present exclusively in one sample) were based on repeated (n = 100) random subsampling of the amplicon data sets. Significant differences in alpha-diversity indices between substrates (i.e. manganese nodules and sediments) were determined by analysis of variance (ANOVA), or by non-parametric Kruskal-Wallis test (KW) when ANOVA's assumptions were not satisfied.

Beta-diversity in samples from different substrates and from the substrate in samples from different sites was quantified by calculating Bray-Curtis dissimilarity based on centred log-ratio (CLR) transformed OTU abundances and Jaccard dissimilarity based on a presence/absence OTU table. The latter was calculated with 100 sequence re-samplings per sample on the smallest dataset (40613 sequences for Bacteria and 1835 sequences for Archaea). Bray-Curtis dissimilarity was used to produce non-metric multidimensional scaling (NMDS) plots, and the Jaccard dissimilarity coefficient was used to calculate the number of shared OTUs between samples. The permutational multivariate analysis of variance (PERMANOVA; Anderson, 2001) was used to test difference in community structure and composition.

Differentially abundant OTUs and genera were detected using the R package ALDEx2 (Fernandes et al. 2014) at a significance threshold of 0.01 and 0.05 for Benjamini–Hochberg (BH) adjusted parametric and non-parametric (KW) P-values, respectively. We only discussed the taxa that were at

https://doi.org/10.5194/bg-2020-11
Preprint. Discussion started: 3 February 2020

least two times more abundant in nodules than in sediments (i.e. (Log2(Nodule/sediment) ≥1) and with a sequences contribution of total number of sequences ≥1 % (for genera) or ≥0.1 % (for OTUs).
All statistical analyses were conducted in R using the core distribution with the additional packages vegan (Oksanen et al. 2015), compositions (Van den Boogaart et al., 2014), iNEXT (Hsieh et al., 2018), and ALDEx2 (Fernandes et al. 2014).

3 Results

3.1 Microbial alpha-diversity

Bacterial and archaeal communities in 5 nodules and 9 sediment samples (Table 1) were investigated using specific sets of primers for Bacteria and Archaea on the same extracted pool of DNA per station. The number of bacterial sequences retrieved from DNA extracted from sediments and nodules was on average 5±5 and 25±14 times higher, respectively, than those obtained for archaea (t-test: $p<0.001$, df=11, t=4.5).
Table 2 shows the statistics of sequence abundance and proportion of singletons and cosmopolitan types. Sequence abundances of bacteria were comparable between sediments and nodules. Cosmopolitan OTU; i.e. those present in 80 % of the sediments and nodule samples were only 9 % of all taxa (77 % of all sequences), whereas rare OTU occurring only in <20 % of all samples represented 50 % the taxa (4 % of all sequences). Sediments *vs* nodules contained only 4 and 2 %, respectively, of endemic taxa, defined as those were abundant in either substrate but rare in the other. Thus the contribution of unique OTUs to the total number of OTUs was lower in manganese nodules than in sediments samples (Table 3, Figure 1a). Bacterial and archaeal diversity was investigated calculating the total number of OTUs (Hill number q=0; H_0) and the estimated richness (Chao1), and the unique OTUs (present exclusively in one station). For this analysis, the latter were calculated with sequence re-sampling, to overcome differences in sequencing depth. Abundance-based coverage estimators, exponential Shannon (Hill number q=1; H_1) and inverse Simpson (Hill number q=2; H_2), were also calculated. The rarefaction curve indicates that the richness (H_0) of the less abundant and rare OTUs was somewhat underestimated both in nodules and in sediments (Figure S1 a-b). However, the bacterial and archaeal diversity was well described for the abundant OTUs (H_1 and H_2; Figure S1 a-b); with more than 90 % of the estimated diversity covered (Figure S1 c-d). Both in sediments and nodules the alpha-diversity indices were higher for Bacteria than for Archaea (t-test: $p<0.0001$, df=12, t=8.0−16.0), while the contribution of unique OTUs to the total number of OTUs was comparable (Table 3). Bacterial communities in manganese nodules have lower Hill numbers and Chao1 indices compared to those associated to sediments (Table 3, Figure 1a). Archaeal communities showed the same patterns for diversity indices and unique OTUs, with exception for H_2 index that did not show significant difference between nodules and sediments (Table 3, Figure 1b).

3.2 Patterns in microbial community composition

The changes in microbial community structure at OTU level (beta-diversity) between substrates and samples were quantified by calculating Bray-Curtis dissimilarities from CLR transformed OTU

https://doi.org/10.5194/bg-2020-11
Preprint. Discussion started: 3 February 2020

abundance. Shared OTUs were estimated by calculating Jaccard dissimilarity from OTU presence/absence based on repeated random subsampling of the amplicon data sets. Microbial communities associated with manganese nodules differed significantly from those found in the sediments (Figure 2, Table S1). Also, significant differences were detected in sediment microbial community structure among the different sites (PERMANOVA; Bacteria: $R^2 = 0.384$; $p = 0.003$; $F_{2,8} = 1.87$; Archaea: $R^2 = 0.480$; $p = 0.013$; $F_{2,8} = 2.31$; Table S1), and between communities associated with nodules and sediment at Reference South (PERMANOVA; Bacteria: $R^2 = 0.341$; $p = 0.023$; $F_{1,6} = 2.59$; Archaea: $R^2 = 0.601$; $p = 0.029$; $F_{1,6} = 7.53$; Table S1). "Site" defined by geographic location, and "Substrate", i.e. origin from sediment or nodule, explained a similar proportion of variation in bacterial community structure (27 % and 23 %, respectively). "Substrate" had a more important role in shaping archaeal communities than "Site" (explained variance 35 % and 19 %, respectively; Table S1). The number of shared OTUs between nodules and sediments (Bacteria: 21 %; Archaea: 19 %) was lower than those shared within nodules (Bacteria: 30 %; Archaea: 30 %) and within sediments (Bacteria: 31 %; Archaea: 32 %) (Figure 4).

Bacterial communities in manganese nodules and sediments were dominated by the classes Gammaproteobacteria (26 %), Aphaproteobacteria (19 %), Deltaproteobacteria (9 %), Bacteroidia (5 %), Acidimicrobiia (4 %), Dehalococcoidia (4 %), Planctomycetacia (4 %), Nitrospinia (3 %), and Phycisphaerae (3 %), which accounted for more than 75 % of the total sequences (Figure 3). All archaeal communities were dominated by Thaumarchaeota (*Nitrosopumilales*), which represented more than 95% of all sequences. The remaining small proportion of sequences was taxonomically assigned to *Woesearchaeia* (Figure 4b). Nodule and sediment samples showed similar compositions of most abundant bacterial genera (contribution to total number of sequence ≥1 %; Figure 4a). 69 bacterial genera (9 % of all genera) were differentially abundant in the nodules and in the sediment, accounting for 36 % and 21 % of total sequences retrieved from nodules and sediments, respectively (ALDEx2: ANOVA adjusted $p<0.01$ and KW adjusted $p<0.05$; Table 4). Of those only one unclassified genus within the family of Sphyngomonadaceae and genus *Filomicrobium* were exclusively found in nodules and not in the sediment samples, and their contribution to the total number of sequences was less than 0.06 %. Genera that were more abundant in the nodules than in the sediments included: unclassified Alphaproteobacteria (7 %), *Nitrospina* (4 %), unclassified SAR324 clade (Marine group B; 3 %), unclassified Hyphomicrobiaceae (3 %), Pirellulaceae Pir4 lineage (2 %), unclassified Methyloligellaceae (1 %), unclassified Pirellulaceae (1 %), *Acidobacteria*, unclassified Subgroup 9 (1 %) and Subgroup 17 (1 %), Nitrosococcaceae *AqS1* (1 %), Calditrichaceae *JdFR-76* (1 %), and *Cohaesibacter* (1 %) (Table 4). In the sediment we identified 21 genera that were more abundant than in the nodules, but all together they represented only 3 % of total sequences recovered from sediments. 128 OTUs were highly abundant in nodules (ALDEx2: ANOVA adjusted $p<0.01$ and KW adjusted $p<0.05$), which accounts for 24 % of total sequences retrieved from nodules (Table 5a). The closest related sequences (≥99 % similarity) were retrieved from ocean crusts (30 %), from nodule fields (26 %), from hydrothermal/seep sediments and deposits (21 %), from worldwide deep-sea sediments (16 %), and associated to invertebrates (7 %; Table 5b and Figure 5).

https://doi.org/10.5194/bg-2020-11
Preprint. Discussion started: 3 February 2020

4 Discussion

Industrial-scale mining of deep-sea polymetallic nodules may remove nodules and the active surface seafloor layer at a spatial scale ranging from ca. 50,000−75,000 km^2 per claim to ca. 1 million km^2 including all current exploration licences (Miller et al., 2018). The regrowth of nodules will take millions of years, thus it is unknown if the associated biota could recover at all (Simon-Lledo et al., 2019). The response of microbial communities to the loss of nodules and seafloor integrity is largely unknown. It may play an important role in the ecological state of the seafloor habitat due to the many functions bacteria and archaea hold in the food-web, element recycling, and biotic interactions, beyond representing the largest biomass in deep-sea sediments (Joergensen and Boetius 2007). It is thus crucial to understand the role of nodules in shaping microbial diversity and in hosting microbes with important ecological functions. So far, only few studies were carried out to investigate the microbiota of nodule fields, and most of them were focused on identifying microbes involved in metal cycling. Here, we investigated similarity of microbial community structures in sediments and nodules retrieved from the Peru Basin. The objectives of this study were: i) to compare the microbes of nodules fields with microbiota of deep-sea sediments, in order to identify specific features of microbial diversity of nodule fields; ii) to elucidate differences in diversity and in microbial community structure between sediments and nodules, and their relapses on potential microbially-mediated functions; iii) to understand the major drivers in shaping microbial communities associated to the nodules.

4.1 Microbial diversity of nodule fields is distinct from other deep-sea areas

Benthic bacterial assemblages in sediments and nodules of the Peru basin showed typical dominance of the classes Gammaproteobacteria, Aphaproteobacteria, Deltaproteobacteria, and Acidimicrobiia, as reported for worldwide deep-sea sediments (Bienhold et al., 2016; Fig. 4) and in the Pacific Nodule Province (Wang et al., 2010; Wu et al., 2013; Shulse et al., 2016; Lindh et al., 2017). But at higher taxonomic resolution we detected substantial differences to the microbial community composition of other deep-sea regions. Sediments of the Peru Basin bacteria classes were depleted in sequence abundances of Flavobacteria, Gemmetimonadetes and Bacilli, whereas sequence abundances of the Chloroflexi (i.e. Dehalococcoidia), Planctomycetes (i.e. Pirellulaceceae, Phycisphaeraceae) and the genus *Nitrospina* were higher compared to other deep-sea regions (Bienhold et al., 2016, Varliero et al., 2019). Dehalococcoidia and Planctomycetes were previously reported as important component of benthic microbial assemblages in the Pacific Ocean (Wang et al., 2010; Wu et al., 2013; Blöthe et al., 2015; Walsh et al., 2016; Lindh et al., 2017). Their contribution to the total community was found to increase in organic matter depleted subsurface sediments (Durbin and Teske, 2011; Walsh et al., 2016).

Dominant OTUs (>1 %) belonged to unclassified Actinomarinales, Gammaproteobacteria, Subgroup 21 (phylum Acidobacteria), and to genus *Woesia* (family Woeseiaceae). Members of Actinomarinales and Woeseiaceae are cosmopolitan types in deep-sea sediments (Bienhold et al., 2016). For Actinomarinales there are no cultivates, and the function of this group remains unknown. In the case of Woeseiaceae, one representative is in culture (*Woeseia ocaeni*). *W. ocaeni* is an obligate chemoorganoheterotroph (Du et al., 2016), suggesting a role in organic carbon remineralization for

https://doi.org/10.5194/bg-2020-11
Preprint. Discussion started: 3 February 2020

members of that family, as recently confirmed by analysis of deep-sea assembled genomes (Hoffmann et al. in revision). Closest related sequences of Subgroup 21 have been reported in deep-sea sediments (Schauer et al. 2010) and across Pacific nodule fields (Wu et al., 2013), but also in association with deep-sea benthic giant foraminifera (Xenophyophores) and in surrounding sediments (Hori et al., 2013). The subgroup 21-like OTU was also one of the 10 most abundant OTUs retrieved from nodules (0.9 %). Xenophyophores have agglutinated tests and can grow to decimetre size, suggesting that members of Subgroup 21 may be colonists of biological and/or hard substrates.

Within the class Alphaproteobacteria the most abundant OTUs (>0.5 %) belonged to unclassified genera of the families Magnetospiraceae (order Rhodospirillales), Hyphomicrobiaceae (order Rhizobiales), and Kiloniellaceae (order Rhodovibrionales). Magnetospiraceae and Hyphomicrobiaceae are the most abundant families in nodules with >2 % of OTUs. Closely related sequences have been reported previously across Pacific Nodule Provinces (Xu et al., 2007; Shulse et al., 2016). The family of Magnetospiraceae includes microaerophilic heterotrophs, able of magnetotaxis and iron reduction (i.e. genus Magnetospirillum; Matsunaga et al. 1991; Schuler and Frankel, 1999), and thus the members of this family could play a role in Fe(III) mobilization, affecting its bioavailability. Hyphomicrobiaceae-like sequences found in this study are related to genera *Hyphomicrobium* and *Pedomicrobium* (sequence identity 97 %), which have been reported to be involved in manganese cycling (Tyler, 1970; Larsen et al., 1999; Stein et al., 2001). A potential contribution of these groups in metal cycling in manganese nodules is also suggested by the presence of closest related sequences in ocean crust (Santelli et al., 2008; Lee et al., 2015), which typically hosts epilithic and endolithic microbial communities of chemolithotrophic metals-oxidizers (Staudigel et al., 2008). Similarly, Kiloniellaceae related OTUs might be involved in metal-cycling as closely related sequences were found in marine basalts (Mason et al., 2007; Santelli et al., 2008) and inside other manganese nodules (Blöthe et al., 2015). Most of the marine cultivates in the family Kiloniellaceae belong to genus *Kiloniella*, that have been isolated from marine macroalga (Wiese et al., 2009), the guts of Pacific white shrimp (Wang et al., 2015), marine sponge (Yang et al., 2015), spider crab and clam (Gerpe et al., 2017), and from the surface water of a polynia in the Western Antarctic Sea (Si et al., 2017). Besides, Kiloniellaceae-like sequences were found in sponges (Cleary et al., 2013), sea start larvae (Galac et al., 2016) and in seamount's iron mats (Scott et al., 2017). The presence of rich sessile and mobile metazoan communities associated to nodules offers various potential hosts for members of Kiloniellaceae. *Kiloniella* is a chemoheterotrophic aerobe, and the draft genome of an isolate from the gut of a Pacific white shrimp shows potential for denitrification and iron acquisition and metabolism (Wang et al., 2015). Thus, either as free-living or host-associated life, the potential contribution of Kiloniellaceae in metal cycling requires further investigation.

Archaea were also present in sediments of the Peru Basin, with Nitrosopumilaceae (phylum Thaumarchaeota) dominating the archaeal communities (Figure 4b). In contrast to what was reported for CCZ (Tully and Heidelberg, 2013; Shulse et al., 2016), Archaeal sequences comprised a lower portion of total sequences retrieved from sediments and nodules of Peru basin (ca. 10 %), and they

https://doi.org/10.5194/bg-2020-11
Preprint. Discussion started: 3 February 2020

were lower in nodules compared to the sediments. The majority of member of Nitrosopumilaceae are believed to be capable of oxidation of ammonia to nitrite, the first step of nitrification (Offre et al., 2013). Archaeal ammonia oxidizers have a higher affinity for ammonia than bacterial ammonia oxidizers, and they are favoured in environments with low ammonia concentrations (Martens-Habbena et al., 2009). The Peru Basin has higher particulate organic-carbon fluxes as compared to central Pacific Ocean (Haeckel et al., 2001; Mewes et al., 2014), which results in higher remineralisation rates and higher ammonia fluxes. These limit the thickness of oxygenated sediments to 10 cm in the Peru Basin while they can reach up to 2-3 m depth in the CCZ (Haeckel et al., 2001; Mewes et al., 2014; Volz et al., 2018). Hence differences observed between CCZ and Peru nodule fields in the contribution of archaeal sequences to microbial assemblages are likely due to ammonia availability, which is controlled by organic matter fluxes.

4.2 Microbial community structure differs between sediments and nodules

Beta-diversity of microbial community structure in the Peru sediments showed remarkable OTU turnover already on a local scale (<60 km; Figure 4), which is at the higher end for turnover rates from previous microbial beta-diversity estimates for bathyal and abyssal seafloor assemblages (Jacob et al., 2013; Ruff et al., 2015; Bienhold et al., 2016; Walsh et al., 2016; Varliero et al., 2019). Here we focused specifically on the contribution of nodules to diversity, which could be a critical parameter in the ecological assessment of nodule removal. Analysis of community composition at OTU level shows that nodules and sediments host distinct bacterial and archaeal communities (Figure 2). Albeit the microbial communities in the sediment showed significant differences between sites, the low number of shared OTUs between sediments and nodules <20% supports the presence of specific bacterial and archaeal communities associated with polymetallic nodule habitats (Wu et al., 2013; Tully and Heidelberg, 2013; Shulse et al., 2016; Lindh et al. 2017). However, the proportion of truly endemic, unique nodule OTUs was also low (Table 3, Figure 1a), nonetheless it is relevant to highlight that nodule removal would lead to a loss of specific types of microbes in a mined deep-sea region (Blöthe et al., 2015).

Microbial communities associated to nodules are generally less diverse than those in the sediments, and the decrease in diversity was observed both in rare and abundant bacterial types (Figure 1 and S1). This seems to be a common feature of polymetallic nodules (Wu et al., 2013; Tully and Heidelberg, 2013; Zhang et al., 2014; Shulse et al., 2016; Lindh et al. 2017). Tully and Heidelberg (2013) suggested that it might be due to less availability of potential energy sources (e.g. organic matter) compared to sediments. Despite that the sedimentation rate exceeds the growth rate of nodules, the nodules are typically exposed to bottom water and not covered by sediments (Peukert et al., 2018). Although, it is unknown whether physical mechanisms (e.g. current regime or seasonal events) or biological processes (e.g. grazing, active cleaning) are responsible for lack of sediments accumulation on nodules, the decrease of microbial diversity with the decrease of organic matter availability is in accordance with positive energy-diversity relationship reported for deep-sea sediments (Bienhold et al., 2012). However, the presence of foraminiferal assemblages (Gooday et al., 2015) and specific sessile

https://doi.org/10.5194/bg-2020-11
Preprint. Discussion started: 3 February 2020

metazoan communities (Vanreusel et al., 2016) on the surface of nodules may represent a potential source of transformed organic matter (e.g. dissolved organic matter) and catabolic products, which may represent a much more valuable energy source for microbes than refractory particulate organic matter sinking from water column. Furthermore, higher microbial diversity in the sediments than in the nodules could be the result of the accumulation of allochthonous microbes, as suggested by the higher proportion of rare and unique OTUs in the sediments. Lastly, the nodules offer hard substrate and presence of metals, which can select for specific Bacteria and Archaea. Similarly, hydrothermal deposits have typically lower bacterial diversity than deep-sea sediments despite chemical energy sources being highly available (Ruff et al., 2015; Wang et al., 2018). We propose that the decreased diversity of abundant OTUs in nodules, observed especially for Bacteria, suggests selection for colonists adapted to specific ecological niches associated with nodules (e.g. high metals concentration, hard substrate, presence of sessile fauna).

4.3 Potential functions of microbial communities associated to nodules

The presence of a large proportion of bacterial community with low abundance in the sediments, but enriched by the nodule environment at the level of genera (35 %) and OTUs (24 %) (Table 4 and 5a) indicates niche specialization. The most abundant OTUs (13 % of bacterial community) in nodules include unclassified Hyphomicrobiaceae, Magnetospiraceae, Alphaproteobacteria, Arenicellaceae and SAR324, *Nitrospina*, *AqS1*, Methyloligellaceae, Subgroup 9, Subgroup 17, Kiloniellaceae, *Cohaesibacter* and JdFR-76, which closest related sequences have been retrieved from Pacific nodules (e.g. Wu et al. 2013; Blöthe et al., 2015), basaltic rocks (e.g. Mason et al 2007; Santelli et al 2008; Mason et al., 2009; Lee et al., 2015), sulfide and carbonate hydrothermal deposits (e.g. Sylvan et al., 2012; Kato et al., 2015), and giant foraminifera (Hori et al., 2013; Table 5b and Figure 5). There are currently no cultivated representatives and metabolic information for these members of the Bacteria, and it is not known whether they have metal tolerance mechanisms or they are actively involved in metal cycling. The high abundance of potential metal reducers (i.e. Magnetospiraceae) and oxidizers (i.e. Hyphomicrobiaceae), and presence of encrusting protozoans (Gooday et al., 2015), microbial eukaryotes (Shulse et al., 2016) and metazoans (Vanreusel et al., 2016) create specific ecological niches, which may be at least partially responsible for the observed selection of microbial taxa in nodules. Overall, these findings suggest that bacterial groups adapted to lithic or biological substrates preferentially colonize nodules, likely favoured by manganese and iron availability, formation of biofilms and presence of sessile fauna communities.

The reduction and dissolution of Mn oxides by dissolved organic matter (e.g. humic compounds) occurs typically in photic or reducing aquatic environments (Sunda et al., 1983; Stone and Morgan, 1984; Stone, 1987; Sunda and Huntsman, 1994). However reductively dissolution of Mn oxides by dissolved organic substrates has been observed also in dark oxygenated seawater (Sunda et al., 1983; Sunda and Huntsman, 1994), suggesting that it could be a relevant abiotic process in manganese nodules. Indeed, this reaction yields manganese(II) and low-molecular-weight organic compounds (Sunda and Kieber, 1994), which potentially may favour Mn-oxidizing Bacteria and microbial exploitation of refractory dissolved organic matter. Intense extracellular enzymatic activities have been

https://doi.org/10.5194/bg-2020-11
Preprint. Discussion started: 3 February 2020

reported for seafloor-exposed basalts (Meyers et al., 2014), raising the question of whether the close related microbes associated to nodules might have comparable degradation rates. Furthermore, nodules host diversified communities of suspension feeders such as serpulid tubeworms, sponges, corals and crinoids (Vanreusel et al., 2016), which filter microbes and POC from the bottom water and release DOM and catabolic metabolites (e.g. ammonia). Thus, nodules may act as hot spots of organic carbon degradation. Albeit metabolic activity has never been quantified on nodules and sequence abundances are lower, the increased abundance of nitrifiers in nodules compared to the sediments reported for Pacific Nodule Province (Tully and Heidelberg, 2013; Shulse et al., 2016) and in this study could indicate a high activity. Nitrifiers catalyse the oxidation of ammonia, a catabolic product of heterotrophic metabolism, to nitrite and eventually to nitrate. In the CCZ the nitrifier community was composed of archaeal ammonia-oxidizing *Nitrosopumilus*, which represented a large portion of the microbial assemblages (up to 20 %), and a minor contribution of bacterial nitrite-oxidizing *Nitrospira* (Tully and Heidelberg, 2013; Shulse et al., 2016). Peru Basin sediments and nodules showed more diversified nitrifier communities, which are enriched by ammonia oxidizing *AqS1* (1 %) and unclassified Nitrosomonadaceae (1 %) and by nitrite-oxidizing *Nitrospina* (4 %) and *Nitrospira* (1 %; Table 4 and 5). *Nitrospina* are not commonly reported for deep-sea sediments, but they are the dominant nitrite oxidizers in the oceans (Luecker et al., 2013). They have recently been reported as symbiont of deep-sea glass sponges (Tian et al., 2016), which also commonly colonize FeMn nodules (Vanreusel et al., 2016). The Nitrospina-related OTUs detected in the nodules showed only low similarity with pelagic *Nitrospina gracilis* and *Nitrospina*-like sequences found in deep-sea glass sponge (sequence identity of 93 %), but were closely related with sequences recovered from marine basalts (Mason et al., 2007; Santelli et al. 2008; Mason et al. 2009), suggesting nodules as a native habitat.

5 Conclusions

The sediments of nodule fields in the Peru Basin host a specific microbial community composition of bacterial taxa reported for organic carbon poor environments (i.e. Chloroflexi, Planctomycetes) and potentially involved in metal-cycling (i.e. Magnetospiraceae, Hyphomicrobiaceae). Nodule communities were distinct from sediments and showed a higher proportion of sequences from potential Mn-cycling bacteria including bacterial taxa found in ocean crust, nodules and hydrothermal deposits. Our results are in general agreement with previous studies in the CCZ, confirming that nodules provide a specific ecological niche. However remarkable differences in community composition (e.g. Mn-cycling bacteria, nitrifiers) between the CCZ and the Peru Basin in microbial community composition also show that environmental setting (i.e. POC flux) and features of FeMn nodules (e.g. metal content) may play a significant role in structuring the nodule microbiome. This indicates that microbial community structure and function would be impacted by nodule removal, and that regional differences would need to be assessed, to determine the spatial turnover and the impact on endemic types.

Furthermore, our results suggest that the removal of nodules, and potentially also the blanketing of nodules with plume sediments suspended during the mining operations may affect the cycling of metal and other elements. Future work is needed to characterize metabolic activities on and in nodules, and to

https://doi.org/10.5194/bg-2020-11
Preprint. Discussion started: 3 February 2020

understand factors and processes controlling nodule colonization. Specifically, restoration experiments should take place to test whether artificial substrates favour the recovery of microbial and fauna communities, and their related ecological functions.

Data availability

Raw sequences with removed primer sequences were deposited at the European Nucleotide Archive (ENA) under accession number PRJEB30517 and PRJEB32680.

Author contributions

A.B, **F.J**, **F.W.** and **M.M** conceived the study. **A.B**, **F.J**, **F.W.** and **T.W.** performed sampling activities. **M.M.** compiled and analysed the data. **M.M.** wrote the paper with the contribution from all Authors.

Competing interest

The authors declare that they have no conflict of interest.

Special issue statement

Acknowledgements

The Authors want to thank captain and crew of the SO242/1 and /2 expedition, and M. Alisch, J. Bäger, J. Barz, A. Nordhausen, F. Schramm, R. Stiens and W. Stiens, (HGF-MPG Joint Research Group on Deep Sea Ecology and Technology) for technical support. The Authors are also grateful to Dr. H. Tegetmeyer for support with Illumina sequencing (CeBiTec laboratory; HGF-MPG Joint Research Group on Deep Sea Ecology and Technology).

This work was funded by the German Ministry of Research and Education (BMBF grant no. 03F0707A-G) as part of the MiningImpact project of the Joint Programming Initiative of Healthy and Productive Seas and Oceans (JPIOceans). We acknowledge further financial support from the Helmholtz Association (Alfred Wegener Institute Helmholtz Center for Polar and Marine Research, Bremerhaven) and the Max Planck Society (MPG), as well as from the ERC Advanced Investigator Grant ABYSS (294757) to AB for technology and sequencing. The research has also received funding from the European Union Seventh Framework Program (FP7/2007- 2013) under the MIDAS project, grant agreement number 603418.

References

Anderson, M. J.: A new method for non-parametric multivariate analysis of variance, Austral Ecol., 26(1), 32–46, 2001.

https://doi.org/10.5194/bg-2020-11
Preprint. Discussion started: 3 February 2020

Bienhold, C., Boetius, A. and Ramette, A.: The energy – diversity relationship of complex bacterial communities in Arctic deep-sea sediments, ISME J., 6, 724–732, doi:10.1038/ismej.2011.140, 2012.

Bienhold, C., Zinger, L., Boetius, A. and Ramette, A.: Diversity and Biogeography of Bathyal and Abyssal Seafloor Bacteria, PLoS One, 11(1), 1–20, doi:10.1371/journal.pone.0148016, 2016.

Blöthe, M., Wegorzewski, A., Müller, C., Simon, F., Kuhn, T. and Schippers, A.: Manganese-Cycling Microbial Communities Inside Deep-Sea Manganese Nodules, Environ. Sci. Technol., 49(13), 7692–7700, doi:10.1021/es504930v, 2015.

Bolger, A. M., Lohse, M. and Usadel, B.: Trimmomatic: a flexible trimmer for Illumina sequence data, Bioinformatics, 30(15), 2114–2120, doi:10.1093/bioinformatics/btu170, 2014.

Boltenkov, B. S.: Mechanisms of formation of deep-sea ferromanganese nodules: Mathematical modeling and experimental results, Geochemistry Int., 50(2), 125–132, doi:10.1134/S0016702911120044, 2012.

Chao, A., J. Gotelli, N., Hsieh, T. C., L. Sander, E., H. Ma, K., Colwell, R. and M. Ellison, A.: Rarefaction and extrapolation with Hill numbers: A framework for sampling and estimation in species diversity studies, Ecol. Monogr., 84, 45–67, doi:10.1890/13-0133.1, 2014.

Chester, R. and Jickells, T.: Marine Geochemistry, 3rd ed Wiley-Blackwell, Oxford., 2012.

Cleary, D. F. R., Becking, L. E., Voogd, N. J. De, Pires, A. C. C., Ana, R. M. P., Egas, C. and Gomes, N. C. M.: Habitat- and host-related variation in sponge bacterial symbiont communities in Indonesian waters, FEMS Microbiol. Ecol., 85, 465–482, doi:10.1111/1574-6941.12135, 2013.

Crerar, D. A. and Barnes, H. L.: Deposition of deep-sea manganese nodules, Geochim. Cosmochim. Acta, 38(2), 279–300, doi:10.1016/0016-7037(74)90111-2, 1974.

Diepenbroek, M., Glöckner, F. O., Grobe, P., Güntsch, A., Huber, R., König-Ries, B., Kostadinov, I., Nieschulze, J., Seeger, B., Tolksdorf, R. and Triebel, D.: Towards an Integrated Biodiversity and Ecological Research Data Management and Archiving Platform : The German Federation for the Curation of Biological Data (GFBio), Inform. 2014 – Big Data Komplexität meistern. GI-Edition Lect. Notes Informatics - Proc., 1711–1724, 2014.

Du, Z., Wang, Z., Zhao, J.-X. and Chen, G.: Woeseia oceani gen. nov., sp. nov., a novel chemoheterotrophic member of the order Chromatiales, and proposal of Woeseiaceae fam. nov, Int. J. Syst. Evol. Microbiol., 66, doi:10.1099/ijsem.0.000683, 2015.

Durbin, A. M. and Teske, A.: Microbial diversity and stratification of South Pacific abyssal marine sediments, Environ. Microbiol., 13(12), 3219–3234, doi:10.1111/j.1462-2920.2011.02544.x, 2011.

Fernandes, A. D., Reid, J. N. S., Macklaim, J. M., McMurrough, T. A., Edgell, D. R. and Gloor, G. B.: Unifying the analysis of high-throughput sequencing datasets: characterizing RNA-seq, 16S rRNA gene sequencing and selective growth experiments by compositional data analysis, Microbiome, 2(1), 15, doi:10.1186/2049-2618-2-15, 2014.

Gerpe, D., Buján, N., Diéguez, A. L., Lasa, A. and Romalde, J. L.: Kiloniella majae sp . nov ., isolated from spider crab (Maja brachydactyla) and pullet carpet shell clam (Venerupis pullastra) ᾳ, Syst. Appl. Microbiol., 40, 274–279, doi:10.1016/j.syapm.2017.05.002, 2017.

Gobet, A., Boetius, A. and Ramette, A.: Ecological coherence of diversity patterns derived from classical fingerprinting and Next Generation Sequencing techniques, Environ. Microbiol., 16(9), 2672–2681, doi:10.1111/1462-2920.12308, 2014.

Gooday, A. J., Goineau, A. and Voltski, I.: Abyssal foraminifera attached to polymetallic nodules from the eastern Clarion Clipperton Fracture Zone: a preliminary description and comparison with North Atlantic dropstone assemblages, Mar. Biodivers., 45(3), 391–412, doi:10.1007/s12526-014-0301-9, 2015.

Halbach, P., Friedrich, G. and von Stackelberg, U.: The manganese nodule belt of the Pacific Ocean. Enke, Stuttgart, p 254, 1988.

Hoffmann, K., Bienhold, C., Buttigieg, P. L., Knittel, K., Laso-Pérez, R., Rapp, J. Z., Boetius, A. and Offre, P.: Diversity and metabolism of Woeseiales bacteria, global members of deep-sea sediment communities. The ISME Journal in revision.

Hori, S., Tsuchiya, M., Nishi, S., Arai, W. and Takami, H.: Active Bacterial Flora Surrounding Foraminifera (Xenophyophorea) Living on the Deep-Sea Floor, Biosci. Biotechnol. Biochem., 77(2), 381–384, doi:10.1271/bbb.120663, 2013.

Hsieh, T.C., Ma, K. H. and Chao, A. iNEXT: iNterpolation and EXTrapolation for species diversity. R package version 2.0.17 URL, 2018: http://chao.stat.nthu.edu.tw/blog/software-download/.

J. Müller, P., Hartmann, M. and Suess, E.: The chemical environment of pelagic sediments, in Halbach P, Friedrich G, von Stackelberg U (eds) The manganese nodule belt of the Pacific ocean: geological, environment, nodule formation, and mining aspects. Enke, Stuttgart, pp. 70–90., 1988.

Jacob, M., Soltwedel, T., Boetius, A. and Ramette, A.: Biogeography of Deep-Sea Benthic Bacteria at Regional Scale (LTER HAUSGARTEN, Fram Strait, Arctic), PLoS One, 8(9), e72779 [online] Available from: https://doi.org/10.1371/journal.pone.0072779, 2013.

Jacobson Meyers, M. E., Sylvan, J. B. and Edwards, K. J.: Extracellular enzyme activity and microbial diversity measured on seafloor exposed basalts from Loihi seamount indicate the importance of basalts to global biogeochemical cycling, Appl. Environ. Microbiol., 80(16), 4854–4864, doi:10.1128/AEM.01038-14, 2014.

Kato, S., Ikehata, K., Shibuya, T., Urabe, T., Ohkuma, M. and Yamagishi, A.: Potential for biogeochemical cycling of sulfur, iron and carbon within massive sulfide deposits below the seafloor, Environ. Microbiol., 17(5), 1817–1835, doi:10.1111/1462-2920.12648, 2015.

KERR, R. A.: Manganese Nodules Grow by Rain from Above, Science (80-.)., 223(4636), 576 LP – 577, doi:10.1126/science.223.4636.576, 1984.

Klindworth, A., Pruesse, E., Schweer, T., Peplies, J., Quast, C., Horn, M. and Glöckner, F. O.: Evaluation of general 16S ribosomal RNA gene PCR primers for classical and next-generation sequencing-based diversity studies, Nucleic Acids Res., 41(1), e1–e1, doi:10.1093/nar/gks808, 2012.

Kuhn, T., Wegorzewski, A., Rühlemann, C. and Vink, A.: Composition, Formation, and Occurrence of Polymetallic Nodules, in Deep-Sea Mining: Resource Potential, Technical and Environmental Considerations, edited by R. Sharma, pp. 23–63, Springer International Publishing, Cham., 2017.

Larsen, E. I., Sly, L. I. and Mcewan, A. G.: Manganese (II) adsorption and oxidation by whole cells and a membrane fraction of Pedomicrobium sp . ACM 3067, Arch. Microbiol., 171(4), 257–264, 1999.

Lee, M. D., Walworth, N. G., Sylvan, J. B., Edwards, K. J. and Orcutt, B. N.: Microbial Communities on Seafloor Basalts at Dorado Outcrop Reflect Level of Alteration and Highlight Global Lithic Clades, Front. Microbiol., 6, 1470, doi:10.3389/fmicb.2015.01470, 2015.

Lindh, M. V., Maillot, B. M., Shulse, C. N., Gooday, A. J., Amon, D. J., Smith, C. R. and Church, M. J.: From the surface to the deep-sea: Bacterial distributions across polymetallic nodule fields in the clarion-clipperton zone of the Pacific Ocean, Front. Microbiol., 8(SEP), 1–12, doi:10.3389/fmicb.2017.01696, 2017.

Luecker, S., Nowka, B., Rattei, T., Spieck, E. and Daims, H.: The Genome of Nitrospina gracilis Illuminates the Metabolism and Evolution of the Major Marine Nitrite Oxidizer , Front. Microbiol. , 4, 27 [online] Available from: https://www.frontiersin.org/article/10.3389/fmicb.2013.00027, 2013.

Mahé, F., Rognes, T., Quince, C., de Vargas, C. and Dunthorn, M.: Swarm: robust and fast clustering method for amplicon-based studies, PeerJ, 2, e593, doi:10.7717/peerj.593, 2014.

Martens-Habbena, W., Berube, P., Urakawa, H., De la Torre, J. and Stahl, D.: Ammonia oxidation kinetics determine niche separation of nitrifying Archaea and Bacteria, Nature, 461, 976–979, doi:10.1038/nature08465, 2009.

Martin, M.: Cutadapt removes adapter sequences from high-throughput sequencing reads, EMBnet.journal; Vol 17, No 1 Next Gener. Seq. Data Anal. - 10.14806/ej.17.1.200 [online] Available from: https://journal.embnet.org/index.php/embnetjournal/article/view/200, 2011.

Mason, O. U., Di Meo-Savoie, C. A., Van Nostrand, J. D., Zhou, J., Fisk, M. R. and Giovannoni, S. J.: Prokaryotic diversity, distribution, and insights into their role in biogeochemical cycling in marine basalts, ISME J., 3(2), 231–242, doi:10.1038/ismej.2008.92, 2009.

Mason, O. U., Stingl, U., Wilhelm, L. J., Moeseneder, M. M., Di Meo-Savoie, C. A., Fisk, M. R. and Giovannoni, S. J.: The phylogeny of endolithic microbes associated with marine basalts, Environ. Microbiol., 9(10), 2539–2550, doi:10.1111/j.1462-2920.2007.01372.x, 2007.

Matsunaga, T.: Applications of bacterial magnets Mognet, Trends Biotechnol., 9(March), 91–95, 1991.

Mewes, K., Mogollón, J. M., Picard, A., Rühlemann, C., Kuhn, T., Nöthen, K. and Kasten, S.: Impact of depositional and biogeochemical processes on small scale variations in nodule abundance in the Clarion‐Clipperton Fracture Zone, Deep Sea Res. Part I Oceanogr. Res. Pap., 91, 125–141, doi:https://doi.org/10.1016/j.dsr.2014.06.001, 2014.

Miller, K. A., Thompson, K. F., Johnston, P. and Santillo, D.: An Overview of Seabed Mining Including the Current State of Development, Environmental Impacts, and Knowledge Gaps, Front. Mar. Sci., 4(January 2018), doi:10.3389/fmars.2017.00418, 2018.

Murray, J. and Renard, A. F.: Report on deep sea deposits based on the specimens collected during the voyage of H.M.S. Challenger in the years 1872 - 1876, Rep. Sci. results Voyag. H.M.S. Chall. Dur. years 1873 - 1876, 1–688, doi:https://doi.org/10.1594/PANGAEA.849018, 1891.

Offre, P., Spang, A. and Schleper, C.: Archaea in biogeochemical cycles. Annu. Rev. Microbiol. 67, 437–457. doi: 10.1146/annurev-micro-092412-155614, 2013.

Oksanen, J., Blanchet, F. G., Kindt, R. et al.: vegan: Community Ecology Package. R package version 2.3-0, 2015.

Peukert, A., Schoening, T., Alevizos, E., Köser, K., Kwasnitschka, T. and Greinert, J.: Understanding Mn-nodule distribution and evaluation of related deep-sea mining impacts using AUV-based hydroacoustic and optical data, Biogeosciences, 15(8), 2525–2549, doi:10.5194/bg-15-2525-2018, 2018.

Pruesse, E., Peplies, J. and Glöckner, F. O.: SINA: Accurate high-throughput multiple sequence alignment of ribosomal RNA genes, Bioinformatics, 28(14), 1823–1829, doi:10.1093/bioinformatics/bts252, 2012.

Riemann, F.: Biological aspects of deep-sea manganese nodule formation, Oceanol. acta, 6(3), 303–311, 1983.

Ruff, S. E., Biddle, J. F., Teske, A. P., Knittel, K., Boetius, A. and Ramette, A.: Global dispersion and local diversification of the methane seep microbiome, Proc. Natl. Acad. Sci., 112(13), 4015 LP – 4020, doi:10.1073/pnas.1421865112, 2015.

Santelli, C. M., Orcutt, B. N., Banning, E., Bach, W., Moyer, C. L., Sogin, M. L., Staudigel, H. and Edwards, K. J.: Abundance and diversity of microbial life in ocean crust, Nature, 453(May), 5–9, doi:10.1038/nature06899, 2008.

Schauer, R., Bienhold, C., Ramette, A. and Harder, J.: Bacterial diversity and biogeography in deep-sea surface sediments of the South Atlantic Ocean, ISME J., 4, 159–170, doi:10.1038/ismej.2009.106, 2010.

Schüler, D. and Frankel, R.: Bacterial magnetosomes: Microbiology, biomineralization and biotechnological applications, Appl. Microbiol. Biotechnol., 52, 464–473, doi:10.1007/s002530051547, 1999.

Scott, J. J., Glazer, B. T. and Emerson, D.: Bringing microbial diversity into focus: high-resolution analysis of iron mats from the Lō'ihi Seamount, Environ. Microbiol., 19(1), 301–316, doi:10.1111/1462-2920.13607, 2017.

Shulse, C. N., Maillot, B., Smith, C. R. and Church, M. J.: Polymetallic nodules, sediments, and deep waters in the equatorial North Pacific exhibit highly diverse and distinct bacterial, archaeal, and microeukaryotic communities, Microbiologyopen, 6(2), 1‐16, doi:10.1002/mbo3.428, 2017.

Si, O., Yang, H., Hwang, C. Y., Kim, S., Choi, S., Kim, J., Jung, M., Kim, S., Roh, S. W. and Rhee, S.: Kiloniella antarctica sp . nov ., isolated from a polynya of Amundsen Sea in Western Antarctic Sea, Int. J. Syst. Evol. Microbiol., 67, 2397–2402, doi:10.1099/ijsem.0.001968, 2017.

Simon-Lledo, E., Bett, B. J., Huvenne, V. A. I., Köser, K., Schoening, T., Greinert, J., and Jones, D. O. B.: Biological effects 26 years after simulated deep-sea mining. Sci. Rep. 9, 8040, doi:10.1038/s41598-019-44492-w, 2019.

Staudigel, H., Furnes, H., McLoughlin, N., Banerjee, N. R., Connell, L. B. and Templeton, A.: 3.5 billion years of glass bioalteration: Volcanic rocks as a basis for microbial life?, Earth-Science Rev., 89(3), 156–176, doi:https://doi.org/10.1016/j.earscirev.2008.04.005, 2008.

Stein, L. Y., Duc, M. T. La, Grundl, T. J. and Nealson, K. H.: Bacterial and archaeal populations associated with freshwater ferromanganous micronodules and sediments, Environ. Microbiol., 3(1), 10–18, 2001.

Sylvan, J. B., Toner, B. M. and Edwards, K. J.: Life and Death of Deep-Sea Vents: Bacterial Diversity and Ecosystem Succession on Inactive Hydrothermal Sulfides, edited by M. A. Moran, MBio, 3(1), e00279-11, doi:10.1128/mBio.00279-11, 2012.

Thiel, H., Schriever, G., Ahnert, A., Bluhm, H., Borowski, C. and Vopel, K.: The large-scale environmental impact experiment DISCOL - Reflection and foresight, Deep. Res. Part II Top. Stud. Oceanogr., 48(17–18), 3869–3882, doi:10.1016/S0967-0645(01)00071-6, 2001.

Tian, R.-M., Sun, J., Cai, L., Zhang, W.-P., Zhou, G., Qui, J.-W. and Qian, P.-Y.: The deep ‐ sea glass sponge Lophophysema eversa harbours potential symbionts responsible for the nutrient conversions of carbon, nitrogen and sulfur, Environ. Microbiol., 18(8), 2481–2494, doi:10.1111/1462-2920.12911, 2016.

Tully, B. J. and Heidelberg, J. F.: Microbial communities associated with ferromanganese nodules and the surrounding sediments, Front. Microbiol., 4(JUN), 1–10, doi:10.3389/fmicb.2013.00161, 2013.

Tyler, P. A.: Hyphomicrobia and the oxidation of manganesse in aquatic ecosystems Mg /, Antonie von Leeuwenhoek, 36, 567–578, 1970.

Van den Boogaart, K. G., Tolosana, R. and Bren, M.: compositions: Compositional Data Analysis. R package version 1.40-1, 2014.

Vanreusel, A., Hilario, A., Ribeiro, P. A., Menot, L. and Arbizu, P. M.: Threatened by mining, polymetallic nodules are required to preserve abyssal epifauna, Sci. Rep., 6, 26808 [online] Available from: https://doi.org/10.1038/srep26808, 2016.

https://doi.org/10.5194/bg-2020-11
Preprint. Discussion started: 3 February 2020

Varliero, G., Bienhold, C., Schmid, F., Boetius, A. and Molari, M.: Microbial Diversity and Connectivity in Deep-Sea Sediments of the South Atlantic Polar Front, Front. Microbiol., 10, 1–18, doi:10.3389/fmicb.2019.00665, 2019.

Volz, J. B., Mogollón, J. M., Geibert, W., Arbizu, P. M., Koschinsky, A. and Kasten, S.: Natural spatial variability of depositional conditions, biogeochemical processes and element fluxes in sediments of the eastern Clarion-Clipperton Zone, Pacific Ocean, Deep. Res. Part I Oceanogr. Res. Pap., 140(December 2017), 159–172, doi:10.1016/j.dsr.2018.08.006, 2018.

Von Stackelberg, U.: Growth history of manganese nodules and crusts of the Peru Basin, Geol. Soc. London, Spec. Publ., 119(1), 153 LP – 176, doi:10.1144/GSL.SP.1997.119.01.11, 1997.

Walsh, E. A., Kirkpatrick, J. B., Rutherford, S. D., Smith, D. C., Sogin, M. and Hondt, S. D.: Bacterial diversity and community composition from seasurface to subseafloor, ISME J., 10, 979–989, doi:10.1038/ismej.2015.175, 2016.

Wang, C., Liao, L., Xu, H., Xu, X., Wu, M. and Zhu, L.: Bacterial Diversity in the Sediment from Polymetallic Nodule Fields of the Clarion-Clipperton Fracture Zone, J. Microbiol., 48(5), 573–585, doi:10.1007/s12275-010-0151-5, 2010.

Wang, L., Li, X., Lai, Q. and Shao, Z.: Kiloniella litopenaei sp . nov ., isolated from the gut microflora of Pacific white shrimp, Litopenaeus vannamei, Antonie Van Leeuwenhoek, 108, 1293–1299, doi:10.1007/s10482-015-0581-5, 2015.

Wang, L., Yu, M., Liu, Y., Liu, J., Wu, Y., Li, L., Liu, J., Wang, M. and Zhang, X.-H.: Comparative analyses of the bacterial community of hydrothermal deposits and seafloor sediments across Okinawa Trough, J. Mar. Syst., 180, 162–172, doi:https://doi.org/10.1016/j.jmarsys.2016.11.012, 2018.

Wang, X. H., Gan, L. and Müller, W. E. G.: Contribution of biomineralization during growth of polymetallic nodules and ferromanganese crusts from the Pacific Ocean, Front. Mater. Sci. China, 3(2), 109–123, doi:10.1007/s11706-009-0033-0, 2009.

Wang, Y. and Qian, P.-Y.: Conservative Fragments in Bacterial 16S rRNA Genes and Primer Design for 16S Ribosomal DNA Amplicons in Metagenomic Studies, PLoS One, 4(10), e7401 [online] Available from: https://doi.org/10.1371/journal.pone.0007401, 2009.

Wegorzewski, A. V. and Kuhn, T.: The influence of suboxic diagenesis on the formation of manganese nodules in the Clarion Clipperton nodule belt of the Pacific Ocean, Mar. Geol., 357, 123–138, doi:10.1016/j.margeo.2014.07.004, 2014.

Wegorzewski, A. V., Kuhn, T., Dohrmann, R., Wirth, R. and Grangeon, S.: Mineralogical characterization of individual growth structures of Mn-nodules with different Ni+Cu content from the central Pacific Ocean, Am. Mineral., 100(11–12), 2497–2508, doi:10.2138/am-2015-5122, 2015.

Wiese, J., Thiel, V., Ga, A., Schmaljohann, R. and Imhoff, J. F.: alphaproteobacterium from the marine macroalga Laminaria saccharina, Int. J. Syst. Evol. Microbiol., 59, 350–356, doi:10.1099/ijs.0.001651-0, 2009.

Wu, Y. H., Liao, L., Wang, C. S., Ma, W. L., Meng, F. X., Wu, M. and Xu, X. W.: A comparison of microbial communities in deep-sea polymetallic nodules and the surrounding sediments in the Pacific Ocean, Deep. Res. Part I Oceanogr. Res. Pap., 79, 40–49, doi:10.1016/j.dsr.2013.05.004, 2013.

Xu, M., Wang, F., Meng, J. and Xiao, X.: Construction and preliminary analysis of a metagenomic library from a deep-sea sediment of east Pacific Nodule Province, FEMS Microbiol. Ecol., 62(3), 233–241, doi:10.1111/j.1574-6941.2007.00377.x, 2007.

Yang, S., Seo, H., Lee, J., Kim, S. and Kwon, K. K.: Kiloniella spongiae sp . nov ., isolated from a marine sponge and emended description of the genus Kiloniella Wiese et al . 2009 and Kiloniella laminariae, Int. J. Syst. Evol. Microbiol., 65, 230–234, doi:10.1099/ijs.0.069773-0, 2015.

Zhang, G., He, J., Liu, F. and Zhang, L.: Iron-Manganese Nodules Harbor Lower Bacterial Diversity and Greater Proportions of Proteobacteria Compared to Bulk Soils in Four Locations Spanning from North to South China, Geomicrobiol. J., 31(7), 562–577, doi:10.1080/01490451.2013.854428, 2014.

Zhang, J., Kobert, K., Flouri, T. and Stamatakis, A.: PEAR: a fast and accurate Illumina Paired-End reAd mergeR, Bioinformatics, 30(5), 614–620, doi:10.1093/bioinformatics/btt593, 2013.

Figure captions

Figure 1. Comparison of diversity indices and unique OTUs between manganese nodules and sediments for (a) bacterial and (b) archaeal communities. H_0: number of OTUs (q=0); H_1: exponential

https://doi.org/10.5194/bg-2020-11
Preprint. Discussion started: 3 February 2020

Shannon (q=1); H_2: inverse Simpson (q=2); Unique: OTUs present exclusively in each station (percentage relative to total OTUs of whole dataset). Chao1 and Unique OTUs were calculated with 100 sequence re-samplings per sample to the smallest dataset (40613 sequences for Bacteria and 1835 sequences for Archaea). Red line shows the median. F: statistic *F-ratio*, with subscript numbers reporting the degrees of freedom between groups and within groups, respectively; p: probability level; KW-test: Kruskal-Wallis test; χ^2: Chi square test value, with subscript numbers reporting the degrees of freedom between groups and sample size, respectively.

Figure 2**.** Non-metric multidimensional scaling (NMDS) plot based on Euclidean distance similarity matrix of bacterial (a) and archaeal (b) community structure at OTU level. Sequence abundances of OTUs were centre log-ratio transformed. Permutational multivariate analysis of variance (PERMANOVA) showed significant differences between nodule and sediment associated microbial communities (for details see Table S1). Each sample (dot) is connected to the weighted averaged mean of the within group distances. Ellipses represent one SD of the weighted averaged mean.

Figure 3. Bacterial community structure at dominant class level (cut-off ≥1 %). MN: manganese nodules; MUC: sediments.

Figure 4. Bacterial (a) and Archaeal (b) dominant genera (cut-off ≥1 %) for surface nodules and sediments. Cluster on top of barplot showed dissimilarity in OTUs composition, as defined by Jaccard dissimilarity index based on presence/absence OTU table and calculated with 100 sequence re-samplings per sample on the smallest dataset (40613 sequences for Bacteria and 1835 sequences for Archaea). un.: unclassified. * due to extremely low number of sequences (n=182), this sample was not included in analysis requiring sequence re-samplings. MN: manganese nodules; MUC: sediments.

Figure 5. Habitats coverage for the closest related sequences (≥99 % similarity) to OTUs highly abundant in the nodules. For details see Table 4a-b.

Table captions

Table 1. Stations list and description of investigated sites/substrates.

Table 2. Statistics of sequence and OTUs abundance, and proportion of absolute singletons, cosmopolitans and endemics for sediments (n=9) and nodule (n=5 for Bacteria, n=4 for Archaea) samples collected in Peru Basin. Absolute singletons: OTUs consisting of sequences occurring only once in the entire dataset; Cosmopolitan: OUTs present in 80 % of sediments and 80 % of nodule samples; Endemics: OTUs exclusively present only in 80 % sediments (and <20 % of nodule samples) or in 80 % nodule samples (and <20 % of sediments samples).

Table 3. Bacterial and archaeal diversity indices and unique OTUs for all nodules and sediment samples. Indices and unique OTUs were calculated without singletons.

https://doi.org/10.5194/bg-2020-11
Preprint. Discussion started: 3 February 2020

Table 4. Genera differentially abundant in nodules and sediments (ALDEx2: glm adjusted $p<0.01$; KW adjusted $p<0.05$). In bold the most abundant genera (≥1 %) at least two times more abundant in nodule than in sediment; in italic the genera exclusively present (i.e. unique) in nodules. Base 2 logarithm of the ratios between geometric mean centred sequences number of nodule (Nod) and sediment (Sed), and average of the sequences contribution of total number of sequences (%) retrieved in nodules and in sediments are shown.

Table 5. (a) OTUs highly abundant in nodules (ALDEx2: glm adjusted $p<0.01$; KW adjusted $p<0.05$). Only OUTs ≥0.1 % are reported. Base 2 logarithm of the ratios between geometric mean centred sequences number of nodule (Nod) and sediment (Sed), and average of the sequences contribution of total number of sequences (%) retrieved in nodules and in sediments are shown. (b) Closest related sequences as indemnified with BLASTn (NCBI nucleotide database 12/06/2019).

https://doi.org/10.5194/bg-2020-11
Preprint. Discussion started: 3 February 2020

Biogeosciences Discussions
Open Access
EGU

Figure 1.

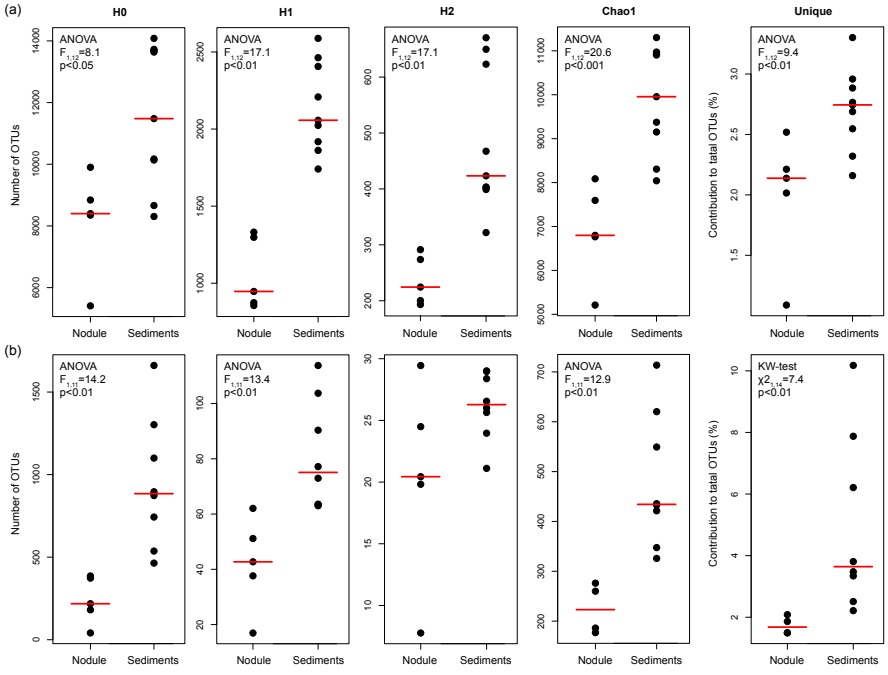

https://doi.org/10.5194/bg-2020-11
Preprint. Discussion started: 3 February 2020

Figure 2.

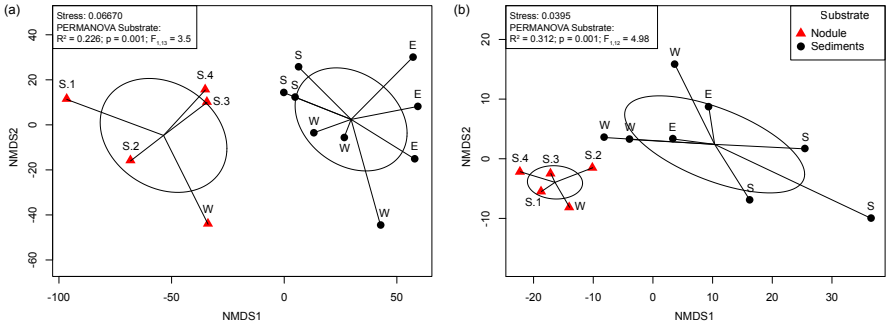

https://doi.org/10.5194/bg-2020-11
Preprint. Discussion started: 3 February 2020

Figure 3.

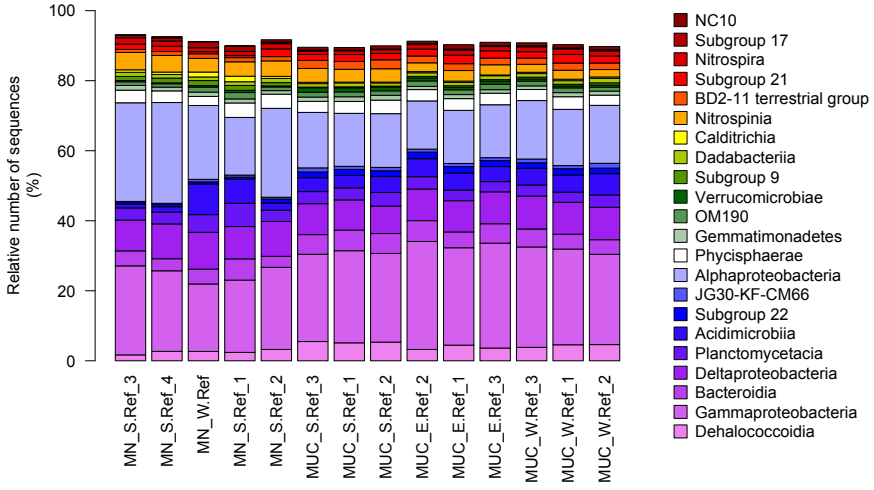

https://doi.org/10.5194/bg-2020-11
Preprint. Discussion started: 3 February 2020

Figure 4.

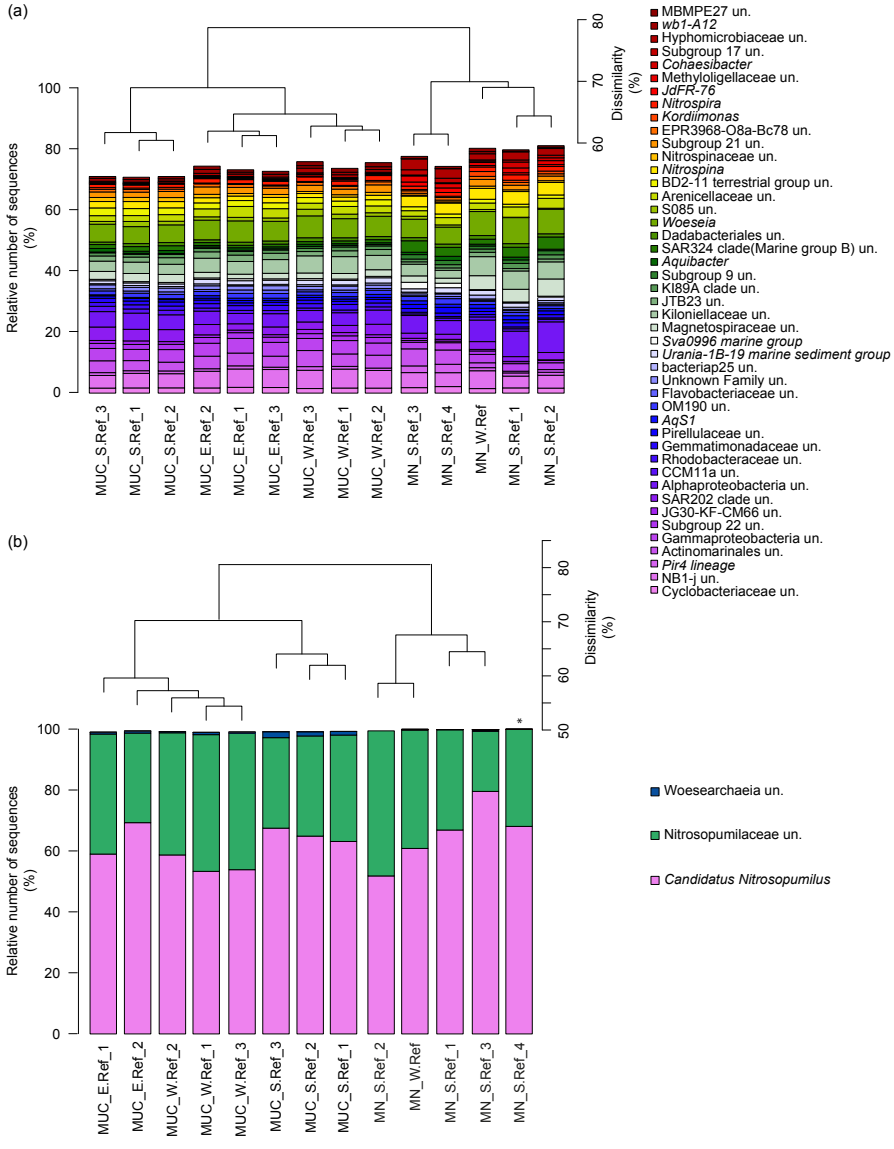

https://doi.org/10.5194/bg-2020-11
Preprint. Discussion started: 3 February 2020

Figure 5.

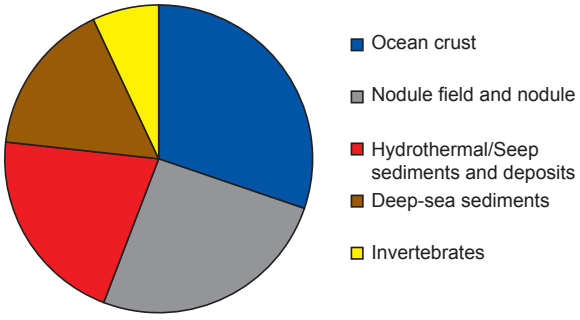

https://doi.org/10.5194/bg-2020-11
Preprint. Discussion started: 3 February 2020

Table 1.

Station	Sample ID	Sampling Time	Latitude (N)	Longitude (E)	Depth (m)	Device	Site	Sediment layer (cm bsf)	Substrate
SO242/2_147	MUC_E.Ref_1	02.09.15	−7.1007	−88.414	4198.2	MUC	Reference East	0-1	sediments
SO242/2_148	MUC_E.Ref_2	02.09.15	−7.1006	−88.414	4195.8	MUC	Reference East	0-1	sediments
SO242/2_151	MUC_E.Ref_3	03.09.15	−7.1006	−88.414	4197.8	MUC	Reference East	0-1	sediments
SO242/2_194	MN_W.Ref	15.09.15	−7.0761	−88.526	4129.5	MUC	Reference West	surface	nodule
SO242/2_194	MUC_W.Ref_1	15.09.15	−7.0761	−88.526	4129.5	MUC	Reference West	0-1	sediments
SO242/2_194	MUC_W.Ref_2	15.09.15	−7.0761	−88.526	4129.5	MUC	Reference West	0-1	sediments
SO242/2_194	MUC_W.Ref_3	15.09.15	−7.0761	−88.526	4129.5	MUC	Reference West	0-1	sediments
SO242/2_198	MN_S.Ref_1	16.09.15	−7.1262	−88.450	4145.6	ROV	Reference South	surface	nodule
SO242/2_198	MN_S.Ref_2	16.09.15	−7.1262	−88.450	4145.6	ROV	Reference South	surface	nodule
SO242-2_208	MN_S.Ref_3	19.09.15	−7.1256	−88.450	4150.7	MUC	Reference South	surface	nodule
SO242-2_208	MN_S.Ref_4	19.09.15	−7.1256	−88.450	4150.7	MUC	Reference South	surface	nodule
SO242/2_208	MUC_S.Ref_1	15.09.15	−7.0761	−88.526	4129.5	MUC	Reference South	0-1	sediments
SO242/2_208	MUC_S.Ref_2	15.09.15	−7.0761	−88.526	4129.5	MUC	Reference South	0-1	sediments
SO242/2_208	MUC_S.Ref_3	15.09.15	−7.0761	−88.526	4129.5	MUC	Reference South	0-1	sediments

MUC: TV-guided MUltiple Corer; ROV: Remote Operated Vehicle (Kiel 6000); bsf: below seafloor.

Table 2.

Bacteria	OTUs n.	OTUs %	Sequences n.	Sequences %
Entire dataset	557468		2271610	
Contaminants	20	0.0	15710	0.7
Absolute singletons	525169	94.2 (56 / 39) [b]	525169	23.1 (14 / 9) [b]
Working dataset [a]	32279	5.8	1730731	76.2
Sediments dataset [a]	28666	5.1 (88.8) [c]	1032246	45.4 (59.6) [c]
Nodule dataset [a]	19279	3.5 (59.7) [c]	698485	30.8 (40.3) [c]
Cosmopolitan OTUs [a]	1452	0.5 (8.9) [c]	1167668	58..4 (76.7) [c]
Endemics OTUs sediments [a]	1356	0.2 (4.2) [c]	39895	1.8 (2.3) [c]
Endemics OTUs nodules [a]	599	0.1 (1.9) [c]	52328	2.3 (3.0) [c]

Archaea	OTUs n.	OTUs %	Sequences n.	Sequences %
Entire dataset	51856		293098	
Contaminants	0	0.0	0	0.0
Absolute singletons	49482	95.4 (77 / 19) [b]	49482	16.9 (14 / 3) [b]
Working dataset [a]	2372	4.6	243616	83.1
Sediments dataset [a]	2356	4.5 (99.3) [c]	219460	74.9 (90.1) [c]
Nodule dataset [a]	591	1.1 (24.9) [c]	24156	8.2 (9.9) [c]
Cosmopolitan OTUs [a]	112	0.2 (4.7) [c]	194736	66.4 (79.9) [c]
Endemics OTUs sediments [a]	198	0.4 (8.3) [c]	10610	3.6 (4.4) [c]
Endemics OTUs nodules [a]	5	0.01 (0.2) [c]	121	0.04 (0.05) [c]

[a] after removal of contaminants (defined by negative control) and absolute singletons sequences (see Materials and Methods for details), percentage calculated on Entire dataset.
[b] contribution of sediments and nodules to absolute singletons, respectively.
[c] percentage calculated on working dataset.

Table 3.

https://doi.org/10.5194/bg-2020-11
Preprint. Discussion started: 3 February 2020

Bacteria	Sequences n. [a]	Sequences n. [b]	H_0	H_1	H_2	Chao1 [c]	sd	Unique (%) [c]	sd
MUC_E.Ref_2	226078	161443	13638	2024	402	10930	201.6	2.7	0.1
MUC_E.Ref_3	218324	166847	13680	2057	423	10972	200.1	2.9	0.1
MUC_E.Ref_1	222924	164985	14082	2208	467	11302	166	3.0	0.1
MN_W.Ref	209563	159724	9902	1296	290	8085	143.6	2.2	0.1
MUC_W.Ref_1	137990	104301	11480	1918	403	9955	164	2.8	0.1
MUC_W.Ref_2	112259	81103	10171	1862	399	9151	148.3	2.3	0.1
MUC_W.Ref_3	236896	178985	13727	1741	322	10905	198.9	3.3	0.1
MN_S.Ref_1	313418	236498	8841	853	192	6798	138.3	2.5	0.1
MN_S.Ref_2	220364	172668	8399	872	199	6766	132.8	2.1	0.1
MN1_S.Ref_3	114074	43932	5409	945	223	5211	73.28	1.1	0.1
MN2_S.Ref_4	64218	76729	8351	1329	272	7594	124.2	2.0	0.1
MUC_S.Ref_1	77424	65890	10137	2588	670	9374	110.5	2.7	0.1
MUC_S.Ref_2	58575	45832	8662	2406	623	8306	93.85	2.2	0.1
MUC_S.Ref_3	59503	40613	8306	2463	650	8041	84.73	2.5	0.1

Archaea	Sequences n. [d]	Sequences n. [b]	H_0	H_1	H_2	Chao1 [c]	sd	Unique (%) [c]	sd
MUC_E.Ref_2	40952	34494	896	63	21	433	52	3.5	0.5
MUC_E.Ref_3	25090	20215	743	73	26	421	50	3.3	0.6
MUC_E.Ref_1	na	na	na	na	na	na	na	na	na
MN_W.Ref	11737	12623	373	51	24	260	33	2.1	0.4
MUC_W.Ref_1	18097	14878	537	63	24	348	36	2.5	0.5
MUC_W.Ref_2	37656	31192	873	77	28	436	53	3.8	0.6
MUC_W.Ref_3	13031	10444	464	64	26	326	31	2.2	0.4
MN_S.Ref_1	7423	5384	218	38	20	186	26	1.5	0.3
MN_S.Ref_2	15314	9472	386	62	29	276	29	1.5	0.4
MN1_S.Ref_3	6099	1835	181	43	20	177	15	1.9	0.3
MN2_S.Ref_4 [e]	722	182	41	17	8	na	na	na	na
MUC_S.Ref_1	34166	29221	1100	90	27	549	66	6.2	0.6
MUC_S.Ref_2	41633	36378	1302	104	29	620	71	7.9	0.8
MUC_S.Ref_3	75344	64433	1661	114	29	714	75	10.2	0.9

H_0: number of OTUs; H_1: exponential Shannon; H_2: inverse Simpson; Unique: OTUs present exclusively in one station (percentage relative to total OTUs of whole dataset); na: not available.

[a] after the merging of forward and reverse reads;

[b] after removal of un-specific and contaminants sequences (see Materials and Methods for details);

[c] calculated with 100 sequence re-samplings per sample to the smallest dataset (40613 sequences for Bacteria and 1835 sequences for Archaea), average data and standard deviation (sd) are given;

[d] after quality trimming of merged forward and reverse reads;

[e] due to extremely low number of sequences, this sample was not included in analyses requiring sequences re-sampling.

https://doi.org/10.5194/bg-2020-11
Preprint. Discussion started: 3 February 2020

Table 4.

Enriched in Nodule	LOG2(Nod/Sed)	Nodule (%)	Sediment (%)
Sphingomonadaceae_unclassified	–	*0.04*	*0.00*
Filomicrobium	–	*0.01*	*0.00*
Geminicoccaceae_unclassified	4	0.12	0.01
Methyloceanibacter	4	0.17	0.02
Robiginitomaculum	4	0.09	0.00
Mesorhizobium	3	0.25	0.01
Cohaesibacter	**3**	**0.78**	**0.10**
OPB56_unclassified	3	0.03	0.00
67-14_unclassified	3	0.31	0.06
Syntrophaceae_unclassified	3	0.06	0.01
Maribacter	3	0.06	0.01
Methyloligellaceae_unclassified	**2**	**1.46**	**0.31**
Entotheonellaceae_unclassified	2	0.20	0.04
Blastocatella	2	0.18	0.04
Calorithrix	2	0.03	0.01
Hyphomicrobiaceae_unclassified	**2**	**2.72**	**0.71**
Planctomicrobium	2	0.05	0.01
Simkaniaceae_unclassified	2	0.13	0.03
Microtrichaceae_unclassified	2	0.13	0.03
LD1-PA32_unclassified	2	0.05	0.01
Subgroup 17_unclassified	**2**	**1.03**	**0.27**
JdFR-76	**2**	**0.93**	**0.26**
Subgroup 9_unclassified	**2**	**1.26**	**0.42**
Chlamydiales_unclassified	2	0.16	0.06
SAR324 clade(Marine group B)_unclassified	**2**	**3.12**	**1.10**
Vermiphilaceae_unclassified	2	0.14	0.05
Acanthopleuribacter	1	0.04	0.01
Bythopirellula	1	0.04	0.01
Nitrospina	**1**	**3.79**	**1.72**
Gemmataceae_unclassified	1	0.04	0.02
Planctomycetacia_unclassified	1	0.05	0.03
SM1A02	1	0.29	0.15
Ekhidna	1	0.17	0.09
Phycisphaeraceae_unclassified	1	0.49	0.27
AqS1	**1**	**1.10**	**0.66**
Microtrichales_unclassified	1	0.19	0.08
Pirellulaceae_unclassified	**1**	**1.31**	**0.75**
pltb-vmat-80_unclassified	1	0.05	0.00
Pir4 lineage	**1**	**1.60**	**0.91**
Alphaproteobacteria_unclassified	**1**	**7.15**	**4.44**
Babeliales_unclassified	1	0.10	0.07
Parvularculaceae_unclassified	1	0.06	0.04
PAUC43f marine benthic group_unclassified	1	0.54	0.36
Subgroup 10	0	0.75	0.67
Aquibacter	0	0.83	0.73
Cyclobacteriaceae_unclassified	0	1.76	1.70
Gemmatimonadaceae_unclassified	0	1.17	1.15
Rhodothermaceae_unclassified	0	0.38	0.39
Total		35.37	17.82

Enriched in Sediment	LOG2(Nod/Sed)	Nodule (%)	Sediment (%)
Planctomycetales_unclassified	-0.02	0.44	0.49
Lutibacter	-1	0.00	0.02
Chloroflexi_unclassified	-2	0.03	0.09
AT-s3-28_unclassified	-2	0.03	0.09
Chitinophagales_unclassified	-2	0.05	0.16
Bacteriovoracaceae_unclassified	-2	0.04	0.14
Nannocystaceae_unclassified	-2	0.02	0.07
Cellvibrionaceae_unclassified	-2	0.02	0.08
OM182 clade_unclassified	-2	0.13	0.47
Candidatus Komeilibacteria_unclassified	-2	0.01	0.03
Roseobacter clade NAC11-7 lineage	-2	0.04	0.11
Bacteroidia_unclassified	-2	0.03	0.11
IS-44	-2	0.05	0.20
Oligoflexaceae_unclassified	-2	0.01	0.08
Lentimicrobiaceae_unclassified	-2	0.01	0.04
Marinoscillum	-3	0.02	0.08
Anaerolineaceae_unclassified	-3	0.05	0.36
Colwelliaceae_unclassified	-3	0.01	0.13
Subgroup 7_unclassified	-3	0.00	0.03
Peredibacter	-3	0.01	0.05
Marinimicrobia (SAR406 clade)_unclassified	-4	0.01	0.07
Total		1.00	2.91

https://doi.org/10.5194/bg-2020-11
Preprint. Discussion started: 3 February 2020

Table 5.

(a)

Phylum	Class	Order	Family	Genus	OTU	LOG2 (Nod/Sed)	Nodule (%)	Sediment (%)
Proteobacteria	Alphaproteobacteria	Rhizobiales	Hyphomicrobiaceae	Hyphomicrobiaceae_unclassified	otu29	2	2.5	0.7
Proteobacteria	Alphaproteobacteria	Rhodospirillales	Magnetospiraceae	Magnetospiraceae_unclassified	otu11	2	2.2	0.7
Proteobacteria	Alphaproteobacteria	Alphaproteobacteria_unclassified	Alphaproteobacteria_unclassified	Alphaproteobacteria_unclassified	otu31	8	1.5	0.0
Proteobacteria	Alphaproteobacteria	Alphaproteobacteria_unclassified	Alphaproteobacteria_unclassified	Alphaproteobacteria_unclassified	otu83	8	0.9	0.0
Proteobacteria	Alphaproteobacteria	Alphaproteobacteria_unclassified	Alphaproteobacteria_unclassified	Alphaproteobacteria_unclassified	otu160	6	0.3	0.0
Proteobacteria	Alphaproteobacteria	Alphaproteobacteria_unclassified	Alphaproteobacteria_unclassified	Alphaproteobacteria_unclassified	otu249	7	0.2	0.0
Proteobacteria	Deltaproteobacteria	SAR324 clade(Marine group B)	SAR324 clade(Marine group B)_unclassified	SAR324 clade(Marine group B)_unclassified	otu66	8	0.7	0.0
Proteobacteria	Deltaproteobacteria	SAR324 clade(Marine group B)	SAR324 clade(Marine group B)_unclassified	SAR324 clade(Marine group B)_unclassified	otu78	2	0.6	0.1
Proteobacteria	Deltaproteobacteria	SAR324 clade(Marine group B)	SAR324 clade(Marine group B)_unclassified	SAR324 clade(Marine group B)_unclassified	otu202	3	0.4	0.0
Proteobacteria	Deltaproteobacteria	SAR324 clade(Marine group B)	SAR324 clade(Marine group B)_unclassified	SAR324 clade(Marine group B)_unclassified	otu317	1	0.2	0.1
Proteobacteria	Deltaproteobacteria	SAR324 clade(Marine group B)	SAR324 clade(Marine group B)_unclassified	SAR324 clade(Marine group B)_unclassified	otu947	4	0.2	0.0
Proteobacteria	Deltaproteobacteria	SAR324 clade(Marine group B)	SAR324 clade(Marine group B)_unclassified	SAR324 clade(Marine group B)_unclassified	otu588	2	0.1	0.0
Proteobacteria	Deltaproteobacteria	SAR324 clade(Marine group B)	SAR324 clade(Marine group B)_unclassified	SAR324 clade(Marine group B)_unclassified	otu425	2	0.1	0.0
Nitrospinae	Nitrospinia	Nitrospinales	Nitrospinaceae	Nitrospina	otu68	3	1.4	0.1
Nitrospinae	Nitrospinia	Nitrospinales	Nitrospinaceae	Nitrospina	otu227	6	0.2	0.0
Nitrospinae	Nitrospinia	Nitrospinales	Nitrospinaceae	Nitrospina	otu215	3	0.2	0.0
Nitrospirae	Nitrospira	Nitrospirales	Nitrospiraceae	Nitrospira	otu636	6	0.2	0.0
Nitrospinae	Nitrospinia	Nitrospinales	Nitrospinaceae	Nitrospina	otu434	3	0.1	0.0
Proteobacteria	Gammaproteobacteria	Arenicellales	Arenicellaceae	Arenicellaceae_unclassified	otu36	2	1.4	0.4
Proteobacteria	Gammaproteobacteria	Arenicellales	Arenicellaceae	Arenicellaceae_unclassified	otu162	5	0.4	0.0
Proteobacteria	Gammaproteobacteria	Steroidobacterales	Woeseiaceae	Woeseia	otu97	4	0.5	0.0
Proteobacteria	Gammaproteobacteria	Steroidobacterales	Woeseiaceae	Woeseia	otu266	2	0.2	0.1
Proteobacteria	Gammaproteobacteria	Steroidobacterales	Woeseiaceae	Woeseia	otu521	6	0.2	0.0
Proteobacteria	Gammaproteobacteria	Steroidobacterales	Woeseiaceae	Woeseia	otu346	4	0.2	0.0
Proteobacteria	Gammaproteobacteria	Steroidobacterales	Woeseiaceae	Woeseia	otu991	5	0.1	0.0
Proteobacteria	Alphaproteobacteria	Rhizobiales	Methyloligellaceae	Methyloligellaceae_unclassified	otu113	2	0.5	0.1
Proteobacteria	Alphaproteobacteria	Rhizobiales	Methyloligellaceae	Methyloligellaceae_unclassified	otu184	7	0.3	0.0
Proteobacteria	Alphaproteobacteria	Rhizobiales	Methyloligellaceae	Methyloligellaceae_unclassified	otu234	3	0.2	0.0
Acidobacteria	Subgroup 9	Subgroup 9_unclassified	Subgroup 9_unclassified	Subgroup 9_unclassified	otu255	6	0.5	0.0
Proteobacteria	Gammaproteobacteria	Nitrosococcales	Nitrosococcaceae	AqS1	otu122	2	0.8	0.3
Acidobacteria	Subgroup 17	Subgroup 17_unclassified	Subgroup 17_unclassified	Subgroup 17_unclassified	otu326	5	0.7	0.0
Acidobacteria	Subgroup 17	Subgroup 17_unclassified	Subgroup 17_unclassified	Subgroup 17_unclassified	otu865	1	0.1	0.1
Calditrichaeota	Calditrichia	Calditrichales	Calditrichaceae	JdFR-76	otu171	1	0.6	0.2
Calditrichaeota	Calditrichia	Calditrichales	Calditrichaceae	JdFR-76	otu541	4	0.2	0.0
Proteobacteria	Alphaproteobacteria	Rhodovibrionales	Kiloniellaceae	Kiloniellaceae_unclassified	otu357	3	0.1	0.0
Proteobacteria	Alphaproteobacteria	Rhodovibrionales	Kiloniellaceae	Kiloniellaceae_unclassified	otu435	4	0.1	0.0
Proteobacteria	Alphaproteobacteria	Rhodovibrionales	Kiloniellaceae	Kiloniellaceae_unclassified	otu370	3	0.1	0.0
Proteobacteria	Alphaproteobacteria	Rhodovibrionales	Kiloniellaceae	Kiloniellaceae_unclassified	otu467	6	0.1	0.0
Proteobacteria	Alphaproteobacteria	Rhodovibrionales	Kiloniellaceae	Kiloniellaceae_unclassified	otu450	2	0.1	0.0
Proteobacteria	Alphaproteobacteria	Rhodovibrionales	Kiloniellaceae	Kiloniellaceae_unclassified	otu519	3	0.1	0.0
Proteobacteria	Alphaproteobacteria	Rhizobiales	Rhizobiaceae	Cohaesibacter	otu71	4	0.7	0.1
Actinobacteria	Acidimicrobiia	Actinomarinales	Actinomarinales_unclassified	Actinomarinales_unclassified	otu163	2	0.3	0.1
Actinobacteria	Acidimicrobiia	Actinomarinales	Actinomarinales_unclassified	Actinomarinales_unclassified	otu532	6	0.2	0.0
Acidobacteria	Subgroup 9	Subgroup 9_unclassified	Subgroup 9_unclassified	Subgroup 9_unclassified	otu342	3	0.3	0.0
Acidobacteria	Subgroup 9	Subgroup 9_unclassified	Subgroup 9_unclassified	Subgroup 9_unclassified	otu674	3	0.1	0.0
Gemmatimonadetes	Gemmatimonadetes	Gemmatimonadales	Gemmatimonadaceae	Gemmatimonadaceae_unclassified	otu203	1	0.4	0.2
Proteobacteria	Alphaproteobacteria	Kordiimonadales	Kordiimonadaceae	Kordiimonas	otu86	2	0.4	0.1
Bacteroidetes	Bacteroidia	Cytophagales	Cyclobacteriaceae	Cyclobacteriaceae_unclassified	otu233	3	0.4	0.0
Dadabacteria	Dadabacteriia	Dadabacteriales	Dadabacteriales_unclassified	Dadabacteriales_unclassified	otu347	3	0.2	0.0
Dadabacteria	Dadabacteriia	Dadabacteriales	Dadabacteriales_unclassified	Dadabacteriales_unclassified	otu1016	3	0.1	0.0
Actinobacteria	Thermoleophilia	Solirubrobacterales	67-14	67-14_unclassified	otu324	3	0.3	0.0
Proteobacteria	Deltaproteobacteria	NB1-j	NB1-j_unclassified	NB1-j_unclassified	otu344	1	0.1	0.0
Planctomycetes	Planctomycetacia	Pirellulales	Pirellulaceae	Pirellulaceae_unclassified	otu538	2	0.1	0.0
Actinobacteria	Acidimicrobiia	Microtrichales	Microtrichaceae	Microtrichaceae_unclassified	otu669	2	0.1	0.0
Acidobacteria	Blastocatellia (Subgroup 4)	Blastocatellales	Blastocatellaceae	Blastocatella	otu489	3	0.1	0.0
Entotheonellaeota	Entotheonellia	Entotheonellales	Entotheonellaceae	Entotheonellaceae_unclassified	otu788	4	0.1	0.0
Acidobacteria	Thermoanaerobaculia	Thermoanaerobaculales	Thermoanaerobaculaceae	Subgroup 10	otu711	3	0.1	0.0
Proteobacteria	Gammaproteobacteria	Oceanospirillales	Kangiellaceae	Kangiellaceae_unclassified	otu744	5	0.1	0.0
Proteobacteria	Gammaproteobacteria	Thiohalorhabdales	Thiohalorhabdaceae	Thiohalorhabdaceae_unclassified	otu571	6	0.1	0.0
Bacteroidetes	Bacteroidia	Cytophagales	Cyclobacteriaceae	Ekhidna	otu651	5	0.1	0.0
Bacteroidetes	Bacteroidia	Flavobacteriales	Flavobacteriaceae	Flavobacteriaceae_unclassified	otu579	6	0.1	0.0
Gemmatimonadetes	BD2-11 terrestrial group	BD2-11 terrestrial group_unclassified	BD2-11 terrestrial group_unclassified	BD2-11 terrestrial group_unclassified	otu1439	3	0.1	0.0

(b)

https://doi.org/10.5194/bg-2020-11
Preprint. Discussion started: 3 February 2020

OTU	NCBI ID ≥ 99% similarity	Habitat(s)
otu29	KT748605.1; JX227334.1; EU491654.1	basaltic crust; nodule fields
otu11	JX227511.1; JQ013353.1; FJ938664.1	nodule fields; deep-sea sediments; cobalt-rich crust
otu31	MG580220.1; KF268757.1	Mariana subduction zone sediments; heavy metal contaminated marine sediments
otu83	MG580220.1; JN621543.1	Mariana subduction zone sediments; manganese oxide-rich marine sediments
otu160	MG580740.1; JX227257.1	Mariana subduction zone sediments; nodule fields
otu249	JQ287236.1; KM051824.1	inactive hydrothermal sulfides; basaltic crust
otu66	JX226721.1 [a]	nodule fields
otu78	JN860354.1; HQ721444.1	hydrothermal vents; deep-sea sediments;
otu202	MG580143.1; JX227690.1; JN860358.1	Mariana subduction zone sediments; nodule fields; hydrothermal vents
otu317	JX227432.1; AY627518.1	nodule fields; deep-sea sediments;
otu947	JX226721.1 [a]	nodule fields
otu588	LC081043.1	nodule
otu425	JX227680.1; FJ938661.1	nodule fields; cobalt-rich crust
otu68	JN886931.1; FJ752931.1; KJ590663.1	hydrothermal carbonate sediments; polychaete burrow environment; biofilm
otu227	MG580382.1; AM997732.1	Mariana subduction zone sediments; deep-sea sediments
otu215	KC901562.1; AB015560.1	basaltic glasses; deep-sea sediments
otu636	HM101002.1; EU491612.1; KC682687.1	Marine Sponge Halichondria; ocean crust;
otu434	EU287401.1; JN977323.1	Subsurface sediments; marine sediments
otu36	JX227383.1; KY977840.1; AM997938.1	nodule fields; Mariana subduction zone sediments; deep-sea sediments
otu162	FN553503.1; AM997671.1	hydrothermal vents; deep-sea sediments
otu97	JX227693.1; FJ024322.1; EU491736.1	nodule fields; ocean crust
otu266	AB694157.1; JX227083.1	deep-sea benthic foraminifera; nodule fields
otu521	KY977757.1; KT336088.1; JX227223.1	Mariana subduction zone sediments; nodules; nodule fields
otu346	KY977757.1; JX227223.1	Mariana subduction zone sediments; nodule fields
otu991	JX227363.1; AM997733.1	nodule fields; deep-sea sediments
otu113	JX226757.1; EU491557.1	nodule fields; ocean crust
otu184	EU491404.1	ocean crust
otu234	EU491604.1	ocean crust
otu255	JX227709.1; FJ437705.1; KM110219.1	nodule fields; hydrothermal deposits
otu122	MG580277.1; AM997814.1; AJ966605.1	Mariana subduction zone sediments; deep-sea sediments; nodule fields
otu326	JN886905.1; KT748584.1	hydrothermal carbonate sediments; basalt crust
otu865	JX227375.1; FJ938651.1; AY225640.1	nodule fields; cobalt-rich crust; hydrothermal sediments
otu171	AM997407.1; FJ205352.1; EU491267.1	deep-sea sediments; hydrothermal vents; ocean crust
otu541	AB694393.1	deep-sea benthic foraminifera
otu357	EU236317.1; GU302472.1	marine sponge; hydrocarbon seep
otu435	KY609381.1; KM051717.1; JX226899.1	Fe-rich hydrothermal deposits; basaltic crust; nodule fields
otu370	EU491648.1 [a]	ocean crust
otu467	FN553612.1; AB858542.1; KM051770.1	hydrothermal vents; sulfide deposits; basaltic crust
otu450	AM997745.1; KM051762.1; EU491108.1	deep-sea sediments; basaltic crust; ocean crust
otu519	GU220747.1; MG580729.1	Fe-rich hydrothermal deposits; Mariana subduction zone sediments
otu71	FJ205181.1; JX226787.1	hydrothermal vents; noduel fields
otu163	JX227427.1; JN886907.1; EU491661.1	nodule fields; hydrothermal carbonate sediments; ocean crust
otu532	EU491402.1; JX227188.1; EU374100.1	ocean crust; nodule fields; deep-sea sediments
otu342	JX227410.1; FJ205219.1; KT336055.1	nodule fields; hydrothermal vents; nodules
otu674	JX227662.1; KT336085.1; FJ938601.1	nodule fields; nodules; cobalt-rich crust
otu203	KP305065.1; FJ938598.1	corals; cobalt-rich crust
otu86	AM997620.1; FJ938474.1	deep-sea sediments; cobalt-rich crust
otu233	JX227464.1; AM997441.1	nodule fields; deep-sea sediments
otu347	JX227062.1; EU491655.1	nodule fields; ocean crust
otu1016	KF616695.1; KM396663.1; EU491261.1	carbonate methane seep; brine seep; ocean crust
otu324	JX226791.1; JN886912.1	nodule fields; hydrothermal carbonate sediments
otu344	EU438185.1; KY977824.1	deep-sea sediments and hydrohtermal vents; ocean crust
otu538	KM356353.1; JX226930.1; DQ996924.1	carbonate methane seep; nodule fields; deep-sea sediments
otu669	EU491619.1; MG580068.1; KT748607.1	ocean crust
otu489	EU491660.1; MG580531.1; AM998023.1	ocean crust; deep-sea sediments
otu788	JN886890.1; MG580099.1	hydrothermal carbonate sediments; ocean crust
otu711	JX193423.1; GU302449.1; AY225643.1	mariculture sediments; hydrocarbon seep; ocean crust
otu744	AB831375.1; EU290406.1; KM454306.1	deep-sea methane-seep sediments; marine sponge; marine sediments
otu571	JQ287033.1; AM911385.1; EU236424.1	hydrothermal sulfides; cold-water corals; sponges
otu651	KT972875.1 [a]	outcrops
otu579	EU491573.1; KT336070.1	ocean crust; nodules
otu1439	JN886922.1; KC747092.1; JN884864.1	hydrothermal carbonate sediments; deep-sea sediments; methane seep

[a] ≥ 98% similarity.